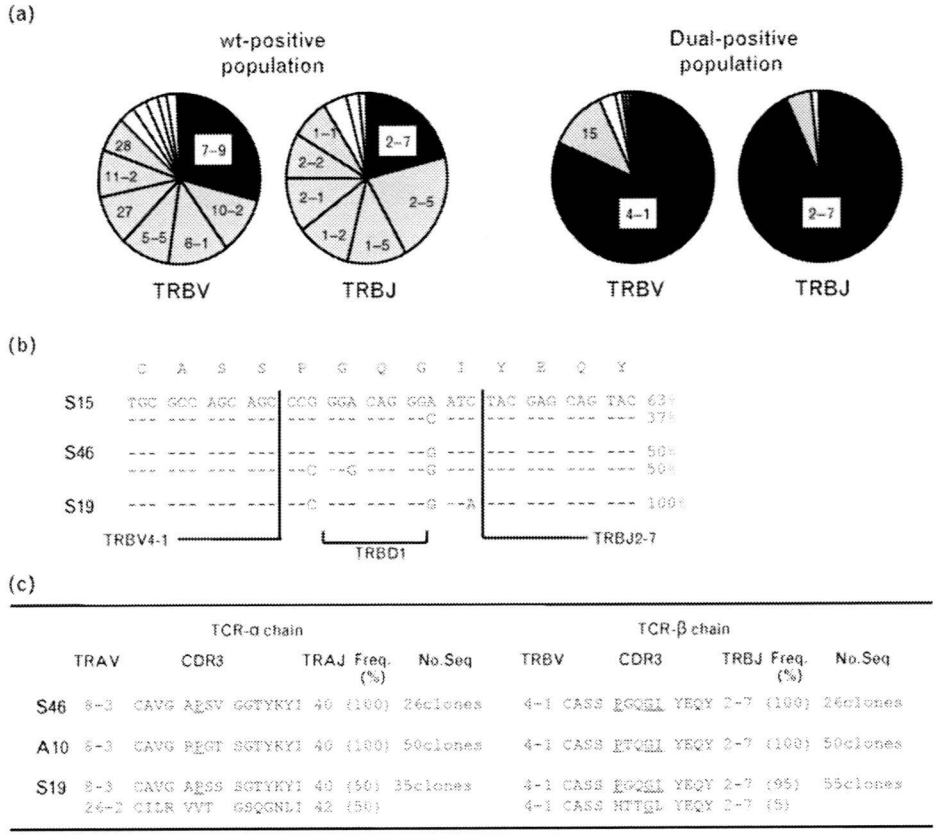

Fig. 4. Characteristics of T-cell receptor β-chain of Nef138-10/A24-tetramer wt-positive and dual-positive CD8$^+$ T-cell populations. Frequencies of TRBV and TRBJ gene usage in CD8$^+$ T cells stimulated with Nef138-10(wt) (Fig. 3) were calculated and shown in a graph. Tet(wt)+/Tet(2F)− (wt-positive)(left) and Tet(wt)+/Tet(2F)+ (dual-positive) (right) populations are shown. The most frequent genes are indicated by black shading, and genes found in more than 5% of the population are indicated by gray shading (a). Nucleotide sequence of CDR3-coding region (CASSPGQGIYEQY) in S15, S46, and S19 was aligned (b). CDR3 amino acid sequence, TRAV, TRAJ, TRBV, and TRBJ usage, and relative frequency of Tet(wt)+/Tet(2F)+ (dual-positive) population in S15, S46, and S19 are shown. Numbers in parenthesis indicate frequency (%) of each clonotype. The consensus amino acid sequences are underlined (c).

could be occurring during in-vitro stimulation by peptides. In order to examine whether the dual-positive population also used TRBV4-1 primarily *in vivo*, frozen PBMCs were thawed and stained with Tet(wt), Tet(2F), and anti-TRBV4-1 antibodies (Fig. 5). PBMCs from patients S15 and T26 had too few dual-positive cells to assess; however, in PBMCs from patients A10 and S19, more than 95% of the dual-positive CD8$^+$ T-cell population were TRBV4-1 positive.

Discussion

Error-prone reverse transcriptase creates the genetic diversity of HIV-1 and serves as an effective means for the virus to evade immune surveillance. Considering the plasticity and hypervariable nature of HIV-1, stereotypic amino acid substitution in the CTL epitope is an enigma that might provide clues to understanding the difficulties encountered in developing effective vaccines for HIV-1. One might predict that point mutations affecting the HIV-1 anchor residues would remove its ability to bind to an MHC heavy chain, resulting in a CTL epitope incapable of eliciting specific CTL response [4]. However, substituted CTL epitopes such as Nef138-10(2F) show the escape phenotype, yet bind to MHC molecules almost as efficiently as the wild-type epitope, with the interaction eliciting strong CD8$^+$ T-cell response [12,13,20].

In this study, we examined the TCR repertoire of CD8$^+$ T cells responding to wt [Nef138-10(wt)] and mutant [Nef138-10(2F)] epitopes. By tetramer dual-staining of A24-positive PBMCs stimulated *in vitro* from HIV-positive patients, we were able to examine two CD8-positive T-cell populations: wt-positive and dual-positive populations. In three patients, the CD8$^+$ T cells could be differentiated according to their relative affinity to Nef138-10(2F)/A24 tetramers (Figs 2 and 3); we designated as 'wt-positive' the population with lower affinity to Nef138-10(2F)/A24 tetramers. Regardless of

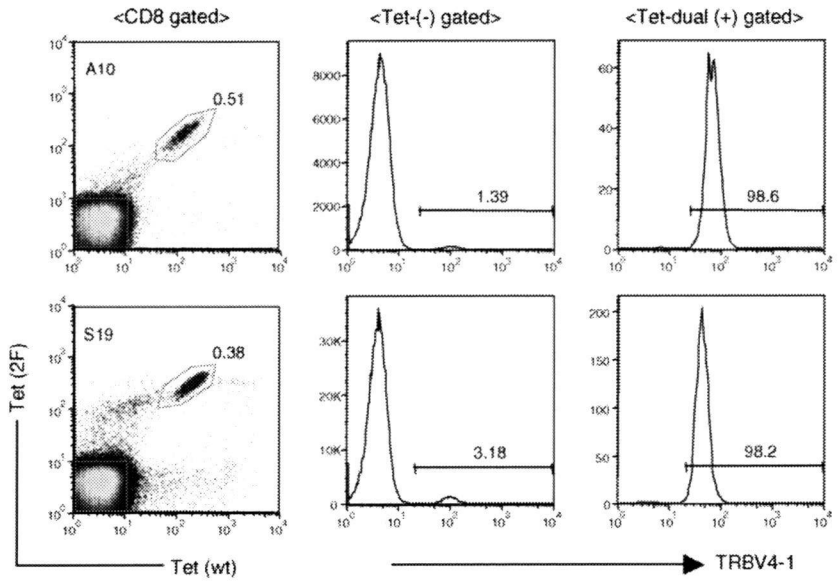

Fig. 5. TRBV4-1 expression in Nef138-10/A24-tetramer dual-positive population *in vivo*. Frozen peripheral blood mononuclear cells from two patients (A10, S19) were stained with Tet(wt) and Tet(2F), anti-CD8 (Pacific Blue), and anti-TRBV4-1(FITC). Tet(wt)+/Tet(2F)+ (dual-positive) and tetramer negative [Tet-(−)] populations are gated. Expression of TRBV4-1 in each population is shown in histogram. FITC, fluorescein isothiocyanate.

which peptide was used for stimulation, the TCR repertoire of the wt-positive population was similar in each patient.

An unexpected finding was that the dual-positive $CD8^+$ T-cell population grown *in vitro* had a highly restricted TCR repertoire compared with the wt-positive $CD8^+$ T-cell population, which showed substantial diversity. Furthermore, the dual-positive $CD8^+$ T-cell population *in vivo* also appeared to have a restricted CTL repertoire in which TRBV4-1 was the predominant clonotype.

Patient I16 appeared to be an exception; in the dual-positive $CD8^+$ T-cell population from this patient, TRBV15 and TRBV10-3 were the major TCR β-chain gene segments. At the time of the study, patient I16 had been followed as an HIV-infected patient in our clinic for at least 8 years, longer than any other study patient. Analysis using frozen PBMCs from patient I16 showed that TRBV4-1/TRBJ2-7 had been the most frequently used clonotype 2 years earlier (data not shown).

In this study, the 2F-positive population was distinguished clearly only in patient T26. Expansion of 2F-positive $CD8^+$ T cells was observed in PBMCs from some of the other patients only following stimulation with much higher peptide concentrations (data not shown). We speculate that 2F-positive $CD8^+$ T cells may require higher amounts of antigen for stimulation and proliferation.

One apparent limitation of our study is that we did not formally prove that the wt single-positive cells are not dual-specific for wt and unknown epitopes, including variant Nef138-10 other than Nef138-10(2F). Although sequencing results showed that the plasma viruses were all Nef138-10(2F) (Fig. 1), we could stimulate and expand $CD8^+$ T cells not only with Nef138-10(2F), but also with Nef138-10(wt) peptides. Our interest is not in the hidden additional specificity of the wt-positive population, but in their relative inability to bind the pMHC to which they must have been exposed *in vivo*. The dual-positive population with higher affinity to Nef138-10(2F)/A24 tetramers had a restricted TCR repertoire. Notably, the patients were viremic even in the presence of CTLs that had a higher affinity against the cognate 'mutant' CTL epitope, Nef138-10(2F)/A24, yet were still able to recognize the cognate 'wt' CTL epitope.

Our data suggest that mutation at the second residue (P2) in the HLA-A24-binding epitope influences T-cell recognition. P2 is the anchor residue of the HLA-A24-binding peptide and dips into the B pocket, forming a hydrogen bond with H70 in the HLA-A24 molecule [21]. A single amino acid substitution from Y to F at a secondary anchor position has been shown to modify the overall conformation of the HLA-A2-restricted HIV Gag-SL9 peptide [22]. However, our recent studies suggest that Y139F substitution in Nef138-10 does not cause a drastic change in pMHC structure (unpublished observation).

Dong *et al.* [23] reported the close correlation between Vβ13.2 usage and long-term nonprogression in four HLA-B8-positive patients. Vβ13.2-positive CTLs were widely reactive to possible escape mutants. In our study, the patients were randomly selected. The relationship between the restricted TCR repertoire and the patient's prognosis is not known, yet we do know that two of the

six treatment-naive patients had CD4 T-cell counts of less than 300 (data not shown). Thus, we infer that the six treatment-naive patients were not necessarily long-term nonprogressors.

The most plausible cause of the restricted TCR repertoire in our case may be lower expression of the Nef138-10(2F) epitope due to impaired or hyper-intracellular processing. We previously examined the killing activity of specific CTL clones against target cells expressing whole Nef protein with or without the 2F mutation (12). Specific killing activity directed against cells expressing Nef protein with the 2F mutation was lower than the activity against cells expressing the wt Nef protein, suggesting that hyper-processing or insufficient processing of Nef protein due to 2F mutation might result in a decrease in cell-surface expression of pMHC molecules. In this situation, CTL with higher avidity might be selected to cope with low antigen expression, resulting in a restricted TCR repertoire of the CTL population. However, the mechanisms enabling the maintenance of strong CTL responses against Nef138-10(2F) *in vitro* are not currently understood. Further studies are needed to show whether the introduction of the 2F mutation actually interferes with processing and leads to a decrease in pMHC molecules on the cell surface.

Previous studies have examined the kinetic association between the emergence of escape variants and the TCR repertoire in HIV-1/SIV infection [24–26]. In acute SIV infection, the emergence of escape viruses was associated with highly conserved TCR β-chain CDR3 motifs, but not with the presence of diverse clonotypic repertoires [24]. We observed viral escape in all patients in this study. We did not detect wild-type viruses even in patients without detectable wt-positive $CD8^+$ T cells. Dual-positive T cells may be enough to remove HIV-1 with the wild-type epitope. Molecular mimicry between wt-pMHC and mutant pMHC may elicit both wt-positive and dual-positive $CD8^+$ T-cell populations whether or not A24-positive patients are infected with wt-positive or mutant HIV-1. The more efficient removal of the wild-type viruses may result from better antigen presentation on the infected cells. Although further evidence is needed, we speculate that impairment of antigen presentation may give viruses with the Nef138-10(2F) mutation a selective advantage in A24-positive patients infected with HIV-1. Not only qualitative, but also quantitative analyses of epitope processing and presentation may shed light on the fundamental mechanism of immune evasion by HIV-1.

Acknowledgements

This work was supported in part by Grant-in-Aid for Scientific Research (B) from Japan Society for the Promotion of Science (JSPS) (33); Grants for AIDS research from the Ministry of Health, Labor, and Welfare of Japan (0616013); a contract research fund from the Ministry of Education, Culture, Sports, Science and Technology (MEXT) for Program of Founding Research Centers for Emerging and Reemerging Infectious Diseases; Strategic Cooperation to Control Emerging and Reemerging Infections funded by the Special Coordination Funds for Promoting Science and Technology of MEXT.

E.M., A.K.-T., and J.-i.N. cloned and sequenced the TCRs. A.K.-T. also wrote the initial draft. M.T. did ELISPOT assays and established epitope-specific $CD8^+$ T-cell lines. T.O. and T.F. were responsible for patient care and contributed to the writing. Y.S. and G.F.G. analyzed the structure of pMHC and TCRs described in this article and contributed to the discussion. A.I. is responsible for the entire study.

This article was presented previously at 4th IAS Conference on HIV Pathogenesis, Treatment and Prevention in 2007 and published as abstract in 'Highly restricted T-cell receptor repertoire against an immunodominant HIV-1 CTL epitope with a stereotypic amino acid substitution'.

References

1. Borrow P, Lewicki H, Hahn BH, Shaw GM, Oldstone MB. **Virus-specific CD8+ cytotoxic T-lymphocyte activity associated with control of viremia in primary human immunodeficiency virus type 1 infection.** *J Virol* 1994; **68**:6103–6110.
2. Koup RA, Safrit JT, Cao Y, Andrews CA, McLeod G, Borkowsky W, *et al.* **Temporal association of cellular immune responses with the initial control of viremia in primary human immunodeficiency virus type 1 syndrome.** *J Virol* 1994; **68**:4650–4655.
3. McMichael AJ, Rowland-Jones SL. **Cellular immune responses to HIV.** *Nature* 2001; **410**:980–987.
4. Goulder PJ, Brander C, Tang Y, Tremblay C, Colbert RA, Addo MM, *et al.* **Evolution and transmission of stable CTL escape mutations in HIV infection.** *Nature* 2001; **412**:334–338.
5. Letvin NL, Walker BD. **Immunopathogenesis and immunotherapy in AIDS virus infections.** *Nat Med* 2003; **9**:861–866.
6. Ammaranond P, Zaunders J, Satchell C, van Bockel D, Cooper DA, Kelleher AD. **A new variant cytotoxic T lymphocyte escape mutation in HLA-B27-positive individuals infected with HIV type 1.** *AIDS Res Hum Retroviruses* 2005; **21**:395–397.
7. Kelleher AD, Long C, Holmes EC, Allen RL, Wilson J, Conlon C, *et al.* **Clustered mutations in HIV-1 gag are consistently required for escape from HLA-B27-restricted cytotoxic T lymphocyte responses.** *J Exp Med* 2001; **193**:375–386.
8. Klenerman P, Rowland-Jones S, McAdam S, Edwards J, Daenke S, Lalloo D, *et al.* **Cytotoxic T-cell activity antagonized by naturally occurring HIV-1 Gag variants.** *Nature* 1994; **369**: 403–407.
9. Leslie AJ, Pfafferott KJ, Chetty P, Draenert R, Addo MM, Feeney M, *et al.* **HIV evolution: CTL escape mutation and reversion after transmission.** *Nat Med* 2004; **10**:282–289.
10. Draenert R, Le Gall S, Pfafferott KJ, Leslie AJ, Chetty P, Brander C, *et al.* **Immune selection for altered antigen processing leads to cytotoxic T lymphocyte escape in chronic HIV-1 infection.** *J Exp Med* 2004; **199**:905–915.
11. Allen TM, Altfeld M, Yu XG, O'Sullivan KM, Lichterfeld M, Le Gall S, *et al.* **Selection, transmission, and reversion of an antigen-processing cytotoxic T-lymphocyte escape mutation in human immunodeficiency virus type 1 infection.** *J Virol* 2004; **78**:7069–7078.

12. Furutsuki T, Hosoya N, Kawana-Tachikawa A, Tomizawa M, Odawara T, Goto M, *et al.* **Frequent transmission of cytotoxic-T-lymphocyte escape mutants of human immunodeficiency virus type 1 in the highly HLA-A24-positive Japanese population.** *J Virol* 2004; **78**:8437–8445.
13. Yokomaku Y, Miura H, Tomiyama H, Kawana-Tachikawa A, Takiguchi M, Kojima A, *et al.* **Impaired processing and presentation of cytotoxic-T-lymphocyte (CTL) epitopes are major escape mechanisms from CTL immune pressure in human immunodeficiency virus type 1 infection.** *J Virol* 2004; **78**: 1324–1332.
14. Milicic A, Price DA, Zimbwa P, Booth BL, Brown HL, Easterbrook PJ, *et al.* **CD8+ T cell epitope-flanking mutations disrupt proteasomal processing of HIV-1 Nef.** *J Immunol* 2005; **175**:4618–4626.
15. Kawana A, Tomiyama H, Takiguchi M, Shioda T, Nakamura T, Iwamoto A. **Accumulation of specific amino acid substitutions in HLA-B35-restricted human immunodeficiency virus type 1 cytotoxic T lymphocyte epitopes.** *AIDS Res Hum Retroviruses* 1999; **15**:1099–1107.
16. Altfeld MA, Trocha A, Eldridge RL, Rosenberg ES, Phillips MN, Addo MM, *et al.* **Identification of dominant optimal HLA-B60- and HLA-B61-restricted cytotoxic T-lymphocyte (CTL) epitopes: rapid characterization of CTL responses by enzyme-linked immunospot assay.** *J Virol* 2000; **74**:8541–8549.
17. Lalvani A, Dong T, Ogg G, Patham AA, Newell H, Hill AV, *et al.* **Optimization of a peptide-based protocol employing IL-7 for in vitro restimulation of human cytotoxic T lymphocyte precursors.** *J Immunol Methods* 1997; **210**:65–77.
18. Kawana-Tachikawa A, Tomizawa M, Nunoya J, Shioda T, Kato A, Nakayama EE, *et al.* **An efficient and versatile mammalian viral vector system for major histocompatibility complex class I/peptide complexes.** *J Virol* 2002; **76**:11982–11988.
19. Folch G, Scaviner D, Contet V, Lefranc MP. **Protein displays of the human T cell receptor alpha, beta, gamma and delta variable and joining regions.** *Exp Clin Immunogenet* 2000; **17**:205–215.
20. Fujiwara M, Tanuma J, Koizumi H, Kawashima Y, Honda K, Mastuoka-Aizawa S, *et al.* **Different abilities of escape mutant-specific cytotoxic T cells to suppress replication of escape mutant and wild-type human immunodeficiency virus type 1 in new hosts.** *J Virol* 2008; **82**:138–147.
21. Cole DK, Rizkallah PJ, Gao F, Watson NI, Boulter JM, Bell JI, *et al.* **Crystal structure of HLA-A*2402 complexed with a telomerase peptide.** *Eur J Immunol* 2006; **36**:170–179.
22. Lee JK, Stewart-Jones G, Dong T, Harlos K, Di Gleria K, Dorrell L, *et al.* **T cell cross-reactivity and conformational changes during TCR engagement.** *J Exp Med* 2004; **200**:1455–1466.
23. Dong T, Stewart-Jones G, Chen N, Esterbrook P, Xu X, Papagno L, *et al.* **HIV-Specific cytotoxic T cells from long-term survivors select a unique T cell receptor.** *J Exp Med* 2004; **200**:1547–1557.
24. Price DA, West SM, Betts MR, Ruff LE, Brenchley JM, Ambrozak DR, *et al.* **T cell receptor recognition motifs govern immune escape patterns in acute SIV infection.** *Immunity* 2004; **21**:793–803.
25. Charini WA, Kuroda MJ, Schmitz JE, Beaudry KR, Lin W, Lifton MA, *et al.* **Clonally diverse CTL response to a dominant viral epitope recognizes potential epitope variants.** *J Immunol* 2001; **167**:4996–5003.
26. Turnbull EL, Lopes AR, Jones NA, Cornforth D, Newton P, Aldam D, *et al.* **HIV-1 epitope-specific CD8+ T cell responses strongly associated with delayed disease progression cross-recognize epitope variants efficiently.** *J Immunol* 2006; **176**:6130–6146.

JOURNAL OF VIROLOGY, Nov. 2009, p. 11569–11580 Vol. 83, No. 22
0022-538X/09/$12.00 doi:10.1128/JVI.00742-09

Loss of the Brm-Type SWI/SNF Chromatin Remodeling Complex Is a Strong Barrier to the Tat-Independent Transcriptional Elongation of Human Immunodeficiency Virus Type 1 Transcripts▽†

Taketoshi Mizutani,[1,3] Aya Ishizaka,[1] Mariko Tomizawa,[2] Takuya Okazaki,[1] Nobutake Yamamichi,[1] Ai Kawana-Tachikawa,[2] Aikichi Iwamoto,[2] and Hideo Iba[1]*

Division of Host-Parasite Interaction, Department of Microbiology and Immunology, Institute of Medical Science, University of Tokyo, Tokyo, Japan[1]; Division of Infectious Disease, Institute of Medical Science, University of Tokyo, 4-6-1 Shirokanedai, Minato-ku, Tokyo 108-8639, Japan[2]; and RNA and Biofunctions, PRESTO, Japan Science and Technology Agency, 4-1-8 Honcho, Kawaguchi, Saitama 332-0012, Japan[3]

Received 10 April 2009/Accepted 26 August 2009

To elucidate the epigenetic regulation of Tat-independent human immunodeficiency virus (HIV) transcription following proviral integration, we constructed an HIV type 1 (HIV-1)-based replication-defective viral vector that expresses a reporter green fluorescent protein (GFP) product from its intact long terminal repeat (LTR). We transduced this construct into human tumor cell lines that were either deficient in or competent for the Brm-type SWI/SNF complex. One day after transduction, single cells that expressed GFP were sorted, and the GFP expression profiles originating from each of these clones were analyzed. Unlike clones of the SWI/SNF-competent cell line, which exhibited clear unimodal expression patterns in all cases, many clones originating from Brm-deficient cell lines either showed a broad-range distribution of GFP expression or were fully silenced. The resorting of GFP-negative populations of these isolated clones showed that GFP silencing is either reversible or irreversible depending upon the proviral integration sites. We further observed that even in these silenced clones, proviral gene transcription initiates to accumulate short transcripts of around 60 bases in length, but no elongation occurs. We found that this termination is caused by tightly closed nucleosome-1 (nuc-1) at the 5′ LTR. Also, nuc-1 is remodeled by exogenous Brm in some integrants. From these results, we propose that Brm is required for the occasional transcriptional elongation of the HIV-1 provirus in the absence of Tat. Since the Brm-type SWI/SNF complex is expressed at marginal levels in resting CD4$^+$ T cells and is drastically induced upon CD4$^+$ T-cell activation, we speculate that it plays crucial roles in the early Tat-independent phase of HIV transcription in affected patients.

Human immunodeficiency virus type 1 (HIV-1) proviral DNA is semirandomly integrated into the host cell genome. The transcription of the HIV-1 provirus is characterized by an early Tat-independent phase and a late Tat-dependent phase. In the early Tat-independent phase, HIV-1 transcription is dependent upon the interaction of host transcription factors with *cis*-regulatory DNA elements with the viral 5′ long terminal repeat (LTR) (23, 26) and the assembly of the transcription apparatus including RNA polymerase II (RNAPII) on these sequences. Importantly, RNAPII synthesizes mostly abortive transcripts during this Tat-independent phase (13, 16). Only a small fraction of the HIV-1 transcripts are in fact expected to be elongated and produce the transactivator Tat protein. Tat and its cellular coactivator, positive transcription factor b (pTEFb), bind the transacting responsive (TAR) element present in the 5′ region of the HIV-1 proviral transcript and cause the hyperphosphorylation of RNAPII, which then elongates this transcript (20, 31). Hence, for the successful elucidation of HIV-1 expression, host factors involved in the first stage of HIV-1 expression will be very important, although the low expression levels of these HIV-1 transcripts may make a detailed analysis difficult.

The SWI/SNF chromatin remodeling complex plays many important roles in epigenetic regulation in human cells. This complex contains either Brm or BRG1 as the catalytic subunit but not both (30). Each of these proteins possesses DNA-dependent ATPase activity, and although they have significant overlapping functions, they do show distinct roles in some biological activities. For example, we previously reported that the Brm-type but not the BRG1-type SWI/SNF complex is required for the stable gene transcription of murine leukemia virus (MLV)-based retrovirus vectors (18) as well as cdx2-dependent villin expression in gastrointestinal cells (36). In Brm-deficient cells, we found that single cells that were transduced with a replication-defective MLV-based vector carrying the *lacZ* reporter frequently formed colonies containing a mixture of LacZ-positive (LacZ$^+$) and LacZ-negative (LacZ$^-$) cells (mosaic colonies). A chromatin immunoprecipitation (ChIP) assay showed that histone deacetylase 1 (HDAC1), HDAC2, and YY1 are recruited around the MLV 5′ LTR when the cells are deficient in Brm (18). It is currently not known whether this requirement of Brm for stable MLV expression is also true for other retroviruses.

In our current study, we examined whether the Brm-type

* Corresponding author. Mailing address: Division of Host-Parasite Interaction, Department of Microbiology and Immunology, University of Tokyo, 4-6-1 Shirokanedai, Minato-ku, Tokyo 108-8639, Japan. Phone: 81-3-5449-5730. Fax: 81-3-5449-5449. E-mail: iba@ims.u-tokyo.ac.jp.

† Supplemental material for this article may be found at http://jvi.asm.org/.

▽ Published ahead of print on 2 September 2009.

SWI/SNF complex is required for stable HIV-1 transcription in the absence of the Tat protein. Using HIV-1-based replication-defective viral vectors, we show that HIV-1 proviral gene expression is destabilized in Brm-deficient cell lines and further that this expression is very often silenced promptly and, in some integrants, can even be reversibly reactivated. We also show that this resulted not from blocks at the level of transcriptional initiation but rather from the suppression of transcriptional elongation. We provide evidence that the Brm-type SWI/SNF chromatin remodeling complex is involved in the disruption of nucleosome-1 (nuc-1), which is present just downstream of the transcription start site, in order to promote the efficient elongation of HIV-1 transcripts.

MATERIALS AND METHODS

Cell culture and preparation of PBMCs. The human cell lines SW13(vim−) (38), C33A, HeLa-S3, HeLa-S3-shBrm4 (37), H1299, AZ521, A204, and 293FT (Invitrogen) were incubated in Dulbecco's modified Eagle's medium with 10% fetal calf serum (Life Technologies/Invitrogen) at 37°C. Peripheral blood mononuclear cells (PBMCs) were obtained from a single healthy donor, purified on Ficoll gradients, and then stained with fluorescein isothiocyanate-conjugated anti-CD4 and phycoerythrin-conjugated anti-HLA-DR antibodies (eBioscience). Monocytes were purified from PBMC cultures by sorting for lymphocytes with dull CD4 and then seeded for 2 days. Proteins were extracted from adherent cells. Resting T cells were purified from PBMCs by sorting for lymphocytes with a high level of expression of CD4 but low levels of HLA-DR. Activated $CD4^+$ T cells were collected as follows: specific antibodies were immobilized on 48-well tissue culture plates by incubating 20 μg/ml anti-CD3 (UCHT1) (eBioscience) and 10 μg/ml anti-CD28 (CD28.2) (eBioscience) in phosphate-buffered saline overnight at 4°C. Excess antibodies were removed from the wells by washing with phosphate-buffered saline. Resting $CD4^+$ T cells were added at 2.5×10^6 cells/well in 0.5 ml of complete RPMI 1640 medium containing 10% fetal calf serum and incubated at 37°C and 5% CO_2. Proteins were collected at 2 days and 6 days after activation. This study was approved by the institutional ethical review board for human investigation at the Institute of Medical Science, University of Tokyo, Tokyo, Japan (approval number 19-27-0131).

Cell sorting and GFP analysis. Cell sorting and flow cytometric analyses were performed using FACSAria and FACSCalibur apparatuses (Becton Dickinson), respectively. For green fluorescent protein (GFP) fluorescence analysis, dead cells were eliminated on the basis of their forward and side scattering using propidium iodide fluorescence.

Plasmids and DNA transfection. The 0.7-kb XhoI-StuI PCR fragment of the NL432 HIV-1 molecular clone (encoding the polypurine tract and the 3′ LTR) (1) was inserted into pLenti6/V5-D-TOPO (Invitrogen) to generate pWL-X. The 3.3-kb BamHI fragment of nlsLacZ (4) and the 0.7-kb fragment of GFP were inserted into the ClaI-XhoI site of pWL-X to generate the constructs pWL-LacZ and pWL-GFP (pWLG), respectively. Plasmids pCAGF1-IRES-Kusabira-Orange (pCAGF1-IKO) (empty vector), pCAGF1-IKO-Brm, and pCAGF1-IKO-Brm (KR) were generated by inserting the 0.7-kb Kusabira Orange fragment of phKO1-MC1 (MBL) into the SmaI-EcoRV site of pCAGF1-IG, pCAGF1-IG-Brm, and pCAGF1-IG-Brm (KR), respectively (37). Oligonucleotides pairs (5′-TTTGGGTCTCTCTGGTTAGACCAGATCTGAGCCTGGGAGCTCTCTGGCTAACTAGGGAACCCACTTTTTTTG-3′ and 5′-AATTCAAAAAAAGTGGGTTCCCTAGTTAGCCAGAGAGCTCCCAGGCTCAGATCTGGTCTAACCAGAGAGACC-3′) were annealed and ligated into vector pmU6 (11) to generate pmU6-62nt. These expression plasmids were transfected into human cell lines using FugeneHD (Roche).

Vector production. Vesicular stomatitis virus G protein-pseudotyped lentiviral vectors (pWL-LacZ and pWL-GFP) were produced using the Virapower lentiviral expression system (Invitrogen).

Mosaic colony assay. A mosaic colony assay was performed essentially as described previously (18). Briefly, cells were transduced with pWL-LacZ at a low multiplicity of infection (MOI) (less than 0.2). At 1 day after transduction, the transduced cultures were trypsinized and seeded at a very low cell density to enable single-colony formation on the plates. Three days after seeding, the cells were assessed for LacZ expression. pCAGF1-IKO and pCAGF1-IKO-Brm were transduced into C33A cells, and 24 h after transfection, Kusabira Orange-positive cells were sorted 1 day before performing the mosaic colony assay.

Genomic and inverse PCRs. Genomic DNAs were extracted from pWLG-transduced cell cultures, and 0.1 μg of these DNA extracts was then used for genomic PCR using the same primer pairs and amplification conditions as those for the ChIP protocol described below. For inverse PCR, genomic DNAs were digested with EcoRI or PstI at 37°C overnight and subjected to self-ligation at 16°C overnight. This facilitated the generation of self-ligated circular DNA carrying both a 5′-terminal proviral fragment (from the 5′ LTR to GFP) and its neighboring genomic sequences. PCR and nested PCR using the following primer sets were then performed to amplify DNA fragments encompassing vector and cellular DNA junctions: primers GFP101 (5′-GTCCGCCCTGAGCAAAGA-3′) and A2 (5′-CAAAGGTCAGTGGATATCTG-3′) for the first PCR and primers A4 (5′-CGATCACATGGTCCTGCTGG-3′) and A3 (5′-CAATCAGGGAAGTAGCCTTG-3′) for nested PCR. Amplified fragments were subjected to sequencing analysis and human genome mapping using BLAST searches.

RT-PCR. Total RNA was prepared from cells using the mirVana microRNA isolation kit (Ambion). Total RNA was treated with DNase (Takara) in accordance with the manufacturer's instructions. Semiquantitative reverse transcription-PCR (RT-PCR) was performed using a Superscript one-step reaction with the Platinum *Taq* kit (Invitrogen). The primer sets used were as follows: start-F (5′-GGGTCTCTCTGGTTAGA-3′) and short-R1 (5′-GGGTTCCCTAGTTAGCC-3′) for the proximal 59 nucleotides (nt), start-F and short-R2 (5′-GGCAAGCTTTATTGAG-3′) for the proximal 86 nt, 5′-TACCGGTCGCCACCATGGTGA-3′ and 5′-GTACTCCAGCTTGTGCCCCAG-3′ for GFP, and 5′-ACCACAGTCCATGCCATCAC-3′ and 5′-TCCACCACCCTGTTGCTGTA-3′ for GAPDH (glyceraldehyde-3-phosphate dehydrogenase). The band intensities were semiquantified by densitometry (Atto Printgraph).

Western blotting. Western blotting was performed as described previously (18) by using antibodies against Brm (Abcam), BRG1 (Santa Cruz Biotechnology), BAF155 (Santa Cruz Biotechnology), BAF60a (BD Transduction Laboratories), HIV-1 p24 (39/5.4A; Abcam), and β-actin (BD Transduction Laboratories).

RNase protection assay. A small RNA fraction (less than 200 nt) was prepared from cells using the mirVana microRNA isolation kit (Ambion). The ^{32}P-labeled HIV-1-specific RNA probe (positions −117 to +86 of the LTR and a non-complementary stretch of 32 nt at the 5′ end) was prepared by in vitro transcription of the antisense probe using T7 RNA polymerase (Invitrogen). Fifteen micrograms of these cellular small RNAs was hybridized overnight with ^{32}P-labeled RNA probes (6×10^5 cpm) at 37°C. An RNase protection assay was performed using the RPAIII kit (Ambion). Protected fragments were electrophoresed on 20% polyacrylamide gels at a high temperature. ^{32}P-end-labeled DynaMarker RNA Low II (BioDynamics Laboratory) RNA markers were also loaded as size standards.

ChIP assay. ChIP assays were performed in accordance with the manufacturer's protocol for the ChIP assay kit (Upstate Biotechnology). The specific antibodies used for immunoprecipitation were anti-Brm (Abcam), anti-BRG1 (Santa Cruz Biotechnology), anti-BAF155 (Santa Cruz Biotechnology), and anti-normal rabbit immunoglobulin G (Santa Cruz Biotechnology). The amplification conditions used for semiquantitative PCR were as follows: 30 cycles of 94°C for 30 s, 60°C for 30 s, and 72°C for 30 s. The primers used were as follows: LTR-F (5′-GAGCTTTCTACAAGGGACTTTCCG-3′) and LTR-R (5′-CCGTGCGCGCTTCAG-3′) (384 bp), CD44-F (5′-TTCGGTCATCCTCTGTCCTGACG-3′) and CD44-R (5′-AATGAGGCTGCCTCGGAAGTTG-3′) (345 bp), and GAPDH-F (5′-TGACTGTCGAACAGGAGGAG-3′) and GAPDH-R (5′-GCTACTAGCGGTTTTACGGG-3′) (174 bp). PCR products were visualized using SYBR green I staining after 5 and 10% polyacrylamide gel electrophoresis. The band intensities were semiquantified by densitometry using the LAS4000UV minisystem (Fuji Film).

Restriction enzyme accessibility assays and ligation-mediated PCR. SW13(vim^-) clones were harvested and resuspended at 2.5×10^6 cells/ml in cold buffer A (10 mM Tris-HCl [pH 7.4], 10 mM NaCl, 3 mM $MgCl_2$, and 0.3 M sucrose) for 5 min and then lysed in 0.3% NP-40 for 3 min. Cellular nuclei were collected by centrifugation (1,500 rpm at 4°C), resuspended in buffer B (10 mM Tris-HCl [pH 7.9], 10 mM $MgCl_2$, 50 mM NaCl, 1 mM dithiothreitol, 100 μg/ml bovine serum albumin, and 0.1 mM phenylmethylsulfonyl fluoride), and digested with 4 U of HindIII and PvuII for 16 h. Genomic DNA was extracted from nuclei with TES buffer (10 mM Tris [pH 8.0], 400 mM NaCl, 2 mM EDTA, and 1% sodium dodecyl sulfate) and treatment with 200 μg/ml proteinase K at 55°C for 5 h. DNA was extracted once with a 1× volume of phenol, followed by a 1:1 phenol-chloroform-isoamyl alcohol extraction and two extractions with 24:1 chloroform-isoamyl alcohol. The ligation-mediated PCR primer used was exactly the same as that described previously (39).

Quantitation of HIV-1 viral production by TNF-α stimulation. ACH-2 and ACH-2-derived cells (1×10^6 cells/24-well plate) were stimulated by TNF-α (10 ng/ml) (R&D Systems) in the presence of 50 μM azidothymidine; culture su-

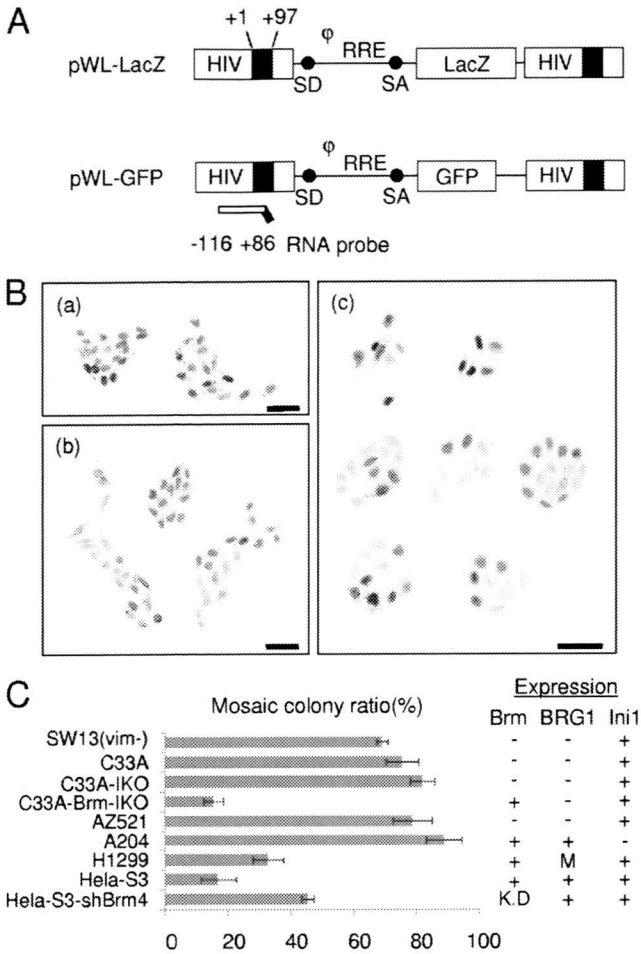

FIG. 1. Prompt silencing of HIV-1-based vector expression occurs in some human cell lines. (A) Schematic representation of vectors pWL-LacZ and pWL-GFP. The position of the RNA probe (nt −116 to +86) used for RNase protection analysis is shown. The vectors contain an intact LTR, from which the *lacZ* or GFP reporter gene is driven from the HIV LTR. SD and SA, splice donor and splice acceptor sites, respectively; RRE, Rev-responsive element, which is necessary to export full-length proviral mRNA from the nucleus to the cytoplasm; ϕ, packaging signal that is necessary for the packaging of full-length vector RNA into the viral particle. (B) Cells were transduced with vector pWL-LacZ at a low MOI (less than 0.2) to minimize the introduction of multiple proviral copies. At 1 day after transduction, the transduced cultures were trypsinized and seeded at a very low cell density to enable single-colony formation. In vector-transduced HeLa-S3 cells (a), positive colonies were mostly observed. HeLa-S3-shBrm4 (b) and C33A (c) cells transduced with the pWL-LacZ vector formed mosaic colonies, as evidenced by the LacZ expression pattern on day 3 after seeding. (C) The mosaic colony ratio was calculated by dividing the mosaic colony number by the sum of the mosaic colony number and the positive colony number. The expression statuses for Brm, BRG1, and Ini1 are summarized at right. K.D and M represent "knockdown" and "mutation," respectively. The error bars indicate the standard deviations (n = 3).

pernatants were then collected by centrifugation at 0, 8, 12, or 24 h poststimulation; and viral production was monitored by HIV-1 p24 antigen enzyme-linked immunosorbent assay (ELISA) (ZeptoMetrix) according to the manufacturer's instructions. The cellular pellets were used for analysis of the cellular p24 protein by Western blotting.

RESULTS

HIV-1 vectors exhibit destabilized reporter expression in Brm-deficient human tumor cell lines. We previously reported, using a mosaic colony assay, that the Brm-type SWI/SNF complex is required for the maintenance of the stable gene expression of MLV-based retrovirus vectors (18). To determine whether this complex is also necessary for the stable transcription of HIV-1 in the absence of Tat, we analyzed the stability of HIV-1 proviral transcription using the same assay. First, we constructed an HIV-1-based LacZ reporter vector under the control of the intact HIV-1 LTR (pWL-LacZ) (Fig. 1A) and transduced this into either SWI/SNF component-competent or Brm-deficient human cells at a low MOI (less than 0.2) to minimize the introduction of multiple proviral copies into a single cell. The transduced cell cultures were grown for 1 day to obtain complete cellular segregation and were then seeded at a low density to enable single-colony formation. The colonies that formed 3 days after seeding were stained for LacZ to assess reporter expression levels (Fig. 1B). When the HIV-1 LacZ vector was transduced into an SWI/SNF-competent cell line such as HeLa-S3, the cells formed colonies in which all the progeny cells expressed LacZ (positive colonies), similar to MLV-based vectors (Fig.1Ba) (18). However, most Brm-deficient colonies were composed of mixed populations of both $LacZ^+$ and $LacZ^-$ cells (mosaic colonies) (Fig.1Bc). When the mosaic colony ratios (the mosaic colony ratio was calculated by dividing the mosaic colony number by the sum of the mosaic colony number and the positive colony number) for several human tumor cell lines were determined, Brm-deficient cell lines such as SW13(vim^-), C33A, and AZ521 exhibited a high ratio. In cell lines competent for the Brm-type SWI/SNF complex, such as HeLa-S3 and H1299 (deficient in BRG1), the mosaic colony ratio was low, as expected, whereas HeLa-S3 cells in which Brm is knocked down (HeLa-S3-shBrm4) showed a higher mosaic colony ratio than the parental HeLa-S3 cells (Fig. 1Bb and C). On the other hand, C33A cells transiently introduced with Brm clearly exhibited a much lower mosaic colony ratio than did those transfected with a control vector (Fig. 1C). A204 cells, which are deficient in Ini1, a core component of the SWI/SNF complex (21), also exhibited a high mosaic colony ratio. These results indicate that the Brm- but not the BRG1-type SWI/SNF complex is required for HIV-1 proviral gene expression in the absence of Tat.

Clonal analysis of HIV-1 LTR expression in Brm-deficient cell cultures. Although a mosaic colony assay using pWL-LacZ is both a convenient and sensitive method for detecting gene silencing within a few days, it cannot sufficiently analyze clonal differences between the integrants in detail or the reversibility of the silencing. To overcome these limitations, the *lacZ* gene was replaced with the GFP gene in the expression viral vector to yield pWLG (GFP reporter vector) (Fig. 1A), which was then introduced into the Brm-deficient cell lines SW13(vim^-) and C33A and the SWI/SNF-competent cell line HeLa-S3. At 1 day after this transduction, single cells expressing GFP were sorted by flow cytometry and then grown for 3 weeks to obtain clonal cultures (see Fig. S1 in the supplemental material).

We obtained 137 clonal cultures: 43 SW13(vim^-), 83 C33A, and 11 HeLa-S3 transductants. All of these clones were con-

firmed to harbor at least one proviral copy by genomic PCR, indicating that cells expressing GFP at least 1 day after transduction were successfully cloned. Among these 137 clones, 46 were randomly selected and further characterized for the copy number of the integrated provirus. Southern blot analysis demonstrated that most clones (average, 84.8%) [16/17 SW13(vim$^-$), 15/21 C33A, and 8/8 HeLa-S3 clones] contained no more than one proviral DNA copy. Since we transduced the GFP reporter vector into cells at an MOI of 0.2 in this experiment, about 9% of the clonal cultures would be predicted to contain more than two integrants using a Poisson distribution of transduction for the entire cellular population (5). This indicated that the experimental results are consistent with theoretical predictions. Although a small degree of contamination by multicopy integrants is unavoidable in this type of experiment, we contend that this does not significantly affect the GFP expression profiles. The representative clones HeLa-S3 clone 4 (HeLa-S3-4); HeLa-S3-20; SW13(vim$^-$)-31, -52, -62, and -78; and C33A-3, -5, -13, and -25, which were used in our closed analysis, however, were confirmed to harbor a single provirus.

All of the transductant clones of the SWI/SNF-competent HeLa-S3 cell line exhibited clear unimodal expression patterns (examples include HeLa-S3-20 and -4) (Fig. 2A, top). Among clones of Brm-deficient cell lines (Fig. 2B and C, top), we found that there were several clones that were fully silenced [SW13(vim$^-$)-31 and -52 and C33A-3 and -13) and many clones for which the GFP expression level ranged broadly from GFP negative (GFP$^-$) to clearly GFP positive (GFP$^+$) [variegated clones, SW13(vim$^-$)-78 and C33A-25]. These tendencies were shown clearly when we plotted the percentages of GFP$^+$ cells in each clone (Fig. 2, middle) and geometrical means of the GFP expression levels of the entire clonal population (Fig. 2, bottom). Here, we expediently defined GFP$^+$ cells as those that have a GFP level higher than that of autofluorescence (M1 gate). These variegated expression profiles observed for Brm-deficient cellular clones are consistent with our observations of mosaic colonies in the LacZ vector-transduced clones (Fig. 1B).

We further analyzed the GFP expression profiles of H1299 cells, which are BRG1 deficient but have intact Brm, and A204 cells, which lack Ini1, an integral component of the SWI/SNF complex. Like HeLa-S3 cells, all of the 42 clones of H1299 cells isolated here showed clear unimodal expression patterns (see Fig. S2 in the supplemental material), whereas A204 clones frequently showed variegated expression of GFP in a manner similar to that of SW13(vim$^-$) and C33A (data not shown). These results indicate that Tat-independent HIV-1 expression is destabilized in the absence of the Brm-type SWI/SNF complex.

To examine the fluctuation of GFP expression in clones such as C33A-25, which shows typical variegated expression, we sorted the GFP$^-$ and GFP$^+$ subpopulations in cultures of C33A-25 cells. By following the time course of the GFP expression patterns in each of these sorted subpopulations, we found that some GFP$^-$ cells became GFP$^+$ and vice versa and that after 3 weeks, each culture showed a broad GFP expression profile that was similar to those of the parental clones (Fig. 3). These results suggest that silencing is reversible in the clones with a broad GFP expression profile. On the other hand, none of the fully silenced clones of SW13(vim$^-$) (clones

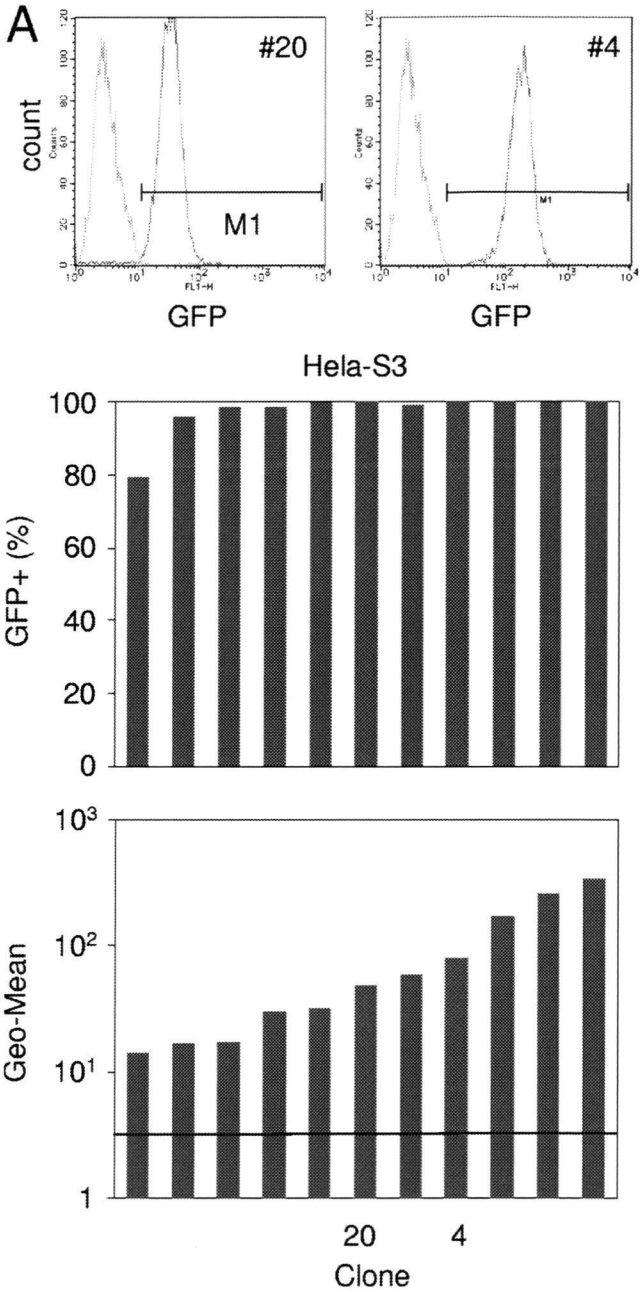

FIG. 2. Single-cell sorting of HIV vector-transduced cells. Vector pWL-GFP was transduced into human cancer cell lines at a low MOI (0.2). At 24 h after transduction, GFP$^+$ cells were single-cell sorted into 96-well plates (FACSAria cell sorting system). Clonal cell lines were analyzed for their GFP expression profiles at 3 weeks after sorting, and fluorescence-activated cell sorter patterns of some representative clones are shown (upper fluorescence-activated cell sorter analysis data and green bar in bar graph). The pink line and green line represent parental cell lines and sorted clones, respectively. The middle bar graph indicates the percentage of GFP$^+$ cells, which were defined as cells within the M1 bar. The bottom bar graph indicates the geometric means (Geo-Mean) of cellular clones of HeLa-S3 (A), SW13(vim$^-$) (B), and C33A (C). The crossbars represent the geometric means of the parental cells (autofluorescence). In these bar graphs, the sorted clones were ordered using geometric means.

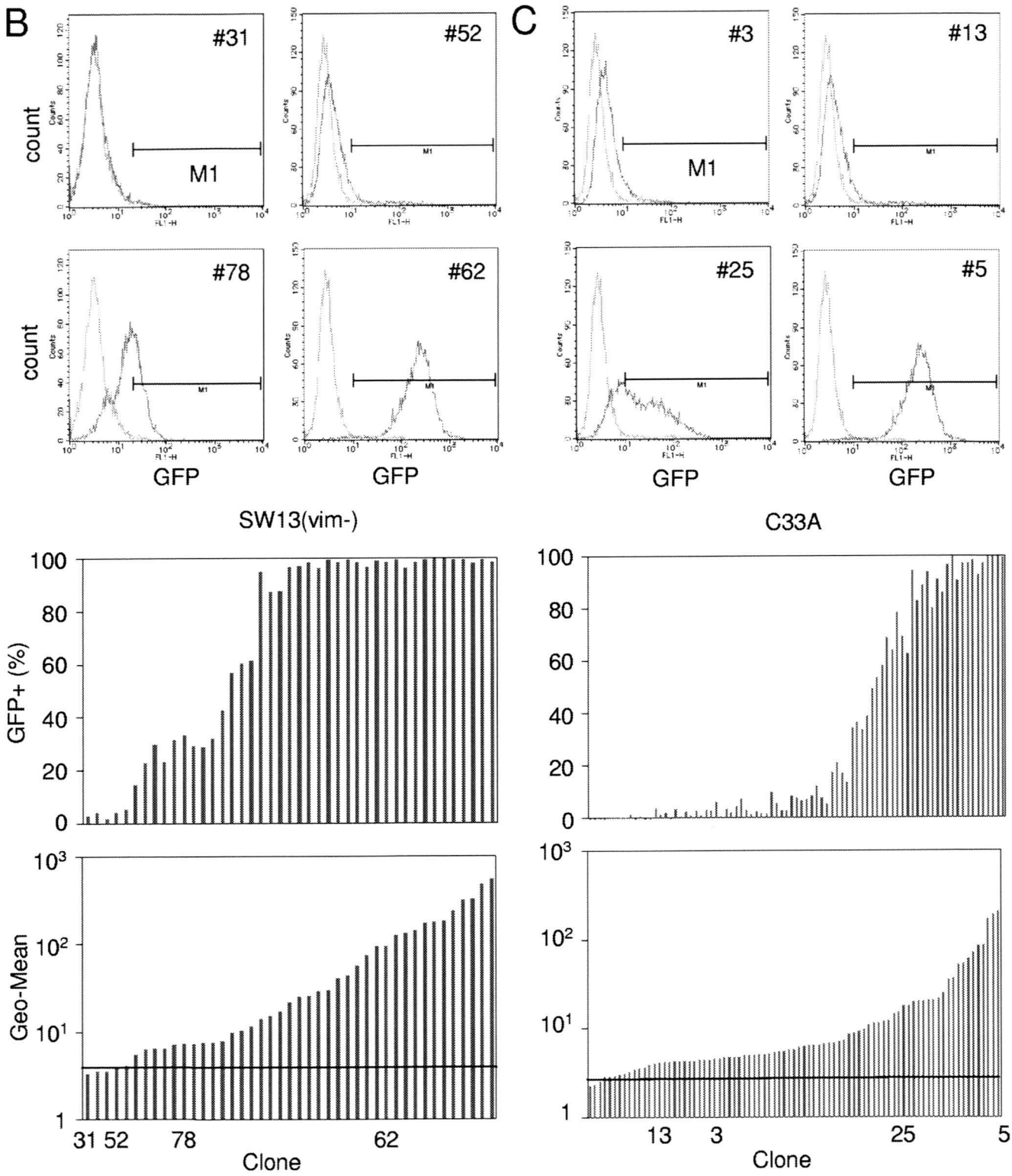

FIG. 2—*Continued.*

31 and 52) or C33A (clones 3 and 13) reexpressed GFP after subsequent growth, indicating that this silencing is irreversible.

We next examined whether GFP expression levels of C33A-25 cells have some correlation with the cell cycle or not. Clone 25 cells were sorted, and their GFP levels and DNA contents (DyeCycle Violet) were simultaneously determined. We compared the GFP expression profile of cells in the G_0/G_1 phase to that of cells in the G_2/M phase. Their GFP expression

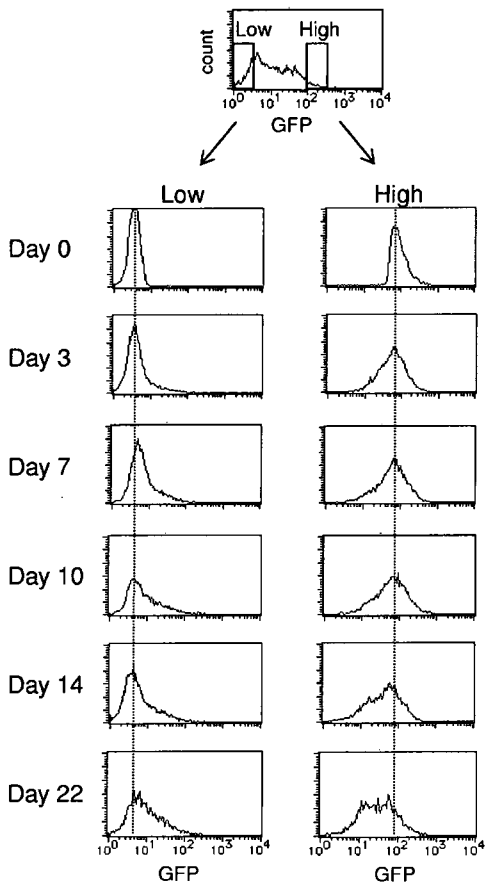

FIG. 3. Time course analysis of the resorting of an HIV vector-transduced clone, C33A-25. Cell fractions from the C33A-25 cellular populations with either low or high GFP expression levels were resorted and grown for about 3 weeks. GFP expression profiles of the aliquots were analyzed on the days indicated.

profiles were very similar, which were also similar to that of the original clone 25 culture (see Fig. S3 in the supplemental material). This result shows that GFP expression levels are not affected by the cell cycle. It was previously reported that CpG methylation could be a mechanism to maintain HIV-1 latency in long-term-infected U937 cells (25). We therefore examined the status of DNA methylation in the LTR region of these cellular clones by using a bisulfate sequencing method. We observed only very a rare and marginal CpG methylation profile in these silenced and variegated clones except for SW13(vim$^-$)-52 cells (see Fig. S4 in the supplemental material). It is notable that both the GFP$^-$ and GFP$^+$ subpopulations in cultures of C33A-25 cells were not methylated like their parental C33A-25 cells. These results indicate that in most cases, our observed silenced or variegated expressions of GFP were not caused by CpG methylation around the HIV promoter region.

By using wild-type HIV-1 and an HIV-1-based vector, it was previously shown that HIV-1 preferentially integrates within introns of coding genes in both human T-cell lines and cancer cell lines and that 60 to 70% of the proviruses integrate into transcription units (24, 35). To elucidate the integration sites in our current sorted clones, we examined the integration sites of several clones of SW13(vim$^-$), C33A, and A204 transductants by inverse PCR and found that most of their integration sites were within the introns of coding genes (Table 1), as was reported previously (24, 35). It is also noteworthy that even though clones such as SW13(vim$^-$)-52 and -76 and C33A-3 and -13 were irreversibly silenced, the proviruses did not reside in heterochromatin. Also, at the same time, we determined the transcriptional orientation of the integrated proviral DNA compared with the host gene where this proviral DNA had integrated but found no obvious causal association (Table 1).

HIV-1 transcripts are not elongated under Brm-deficient conditions. To gain further insight into the role of Brm in HIV-1 transcription, we wished to examine the transcriptional steps during HIV-1 promoter transcription that were restricted in Brm-deficient cells. It was reported previously that only a small fraction of the initial HIV-1 transcripts are fully elongated in the absence of Tat. Whereas the major transcripts produced in this early phase seem to be prematurely terminated, this would eventually lead to an accumulation of Tat and a trigger of drastic late-phase transcription (13, 17). Hence, we first examined whether transcription is initiated in GFP-silenced Brm-deficient clones. Transcriptional initiation and elongation of the HIV-1 vector were assayed by RT-PCR using primer pairs that cover the transcriptional start site and the GFP gene (Fig. 4A). Although no amplified band corre-

TABLE 1. Chromosomal features associated with the integration sites of HIV-1 vector pWLG in cellular clones

Clone	GFP expression profile	Chromosomal locus	Location of integration site (gene name)	Provirus direction vs host gene
SW13(vim−)-31	Silenced	—[a]		
SW13(vim−)-43	Broad	Chr6q22.31	Intronic (RNF217)	Reverse
SW13(vim−)-49	Expressing	Chr5q21	Intergenic	
SW13(vim−)-52	Silenced	Chr.2p13	Intronic (ZNF638)	Reverse
SW13(vim−)-63	Broad	Chr9p24.1	Intronic (NFIB)	Forward
SW13(vim−)-68	Expressing	Chr.9q32	Intronic (KIAA1958)	Reverse
SW13(vim−)-76	Silenced	Chr.1q41	Intronic (C1orf80)	Forward
SW13(vim−)-77	Expressing	Chr.21q22.3	Intronic (PCNT)	Reverse
SW13(vim−)-78	Broad	Chr.16p13.3	Intergenic	
C33A-3	Silenced	Chr.11p11.2	Intronic (C11orf49)	Reverse
C33A-13	Silenced	Chr.11q13	Intronic (DPH4)	Forward
A204-7	Broad	Chr.1p36.1	Intergenic	

[a] —, Integrated into a highly repetitive sequence. The exact locus cannot be identified.

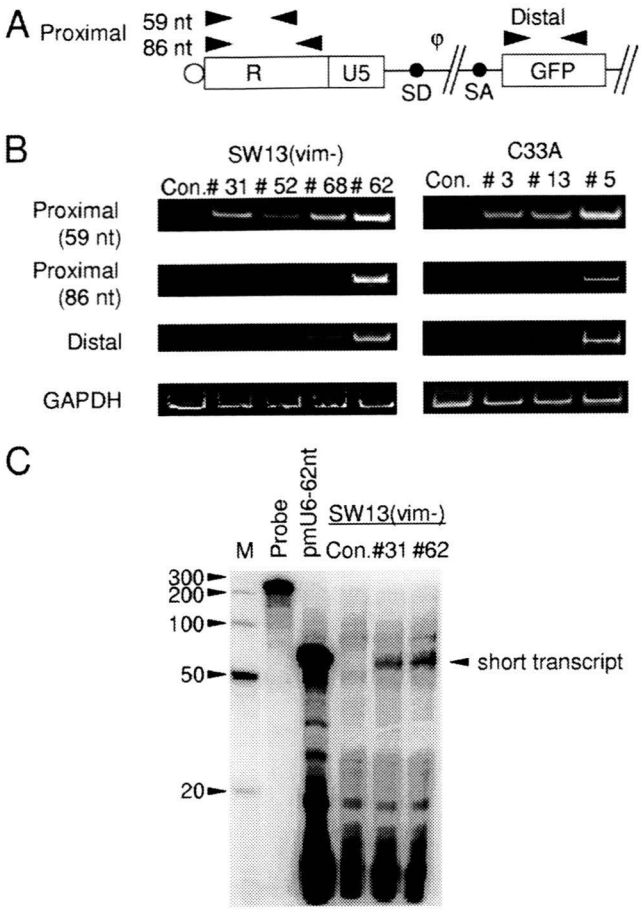

FIG. 4. Analysis of RNA transcripts in the pWLG-transduced cell clones. (A) Schematic of the pWL-GFP vector showing the location of RT-PCR primers (arrowheads). The proximal primers amplify both abortive and full-length products (R region of the 5′ LTR and the 3′ LTR) of transcription. The distal primer amplifies any full-length product of transcription. SD and SA, splice donor and splice acceptor sites, respectively. (B) Expression levels of the proviral transcripts were measured in the clones SW13(vim$^-$)-31, -52, -68, and -62 and C33A-3, -13, and -5 as well as the parental cell lines SW13(vim$^-$) and C33A by semiquantitative RT-PCR. Con., control. (C) RNase protection analysis of the clones SW13(vim$^-$)-31 and -62. The RNA probe used is described in the legend of Fig. 1A. Fifteen micrograms of small RNA extracts was used and hybridized with this probe at 37°C. Protected RNA fragments were resolved using 20% denaturing acrylamide gel electrophoresis at a high temperature. As a positive control, 62 nt of the TAR stem-loop region of HIV-1 transcripts driven by a mouse polymerase III type U6 promoter (pmU6-62nt) was used.

sponding to the GFP gene (the distal portion of transcript) was detected in GFP-silenced SW13(vim$^-$)-31 and -52 and C33A-3 and -13 cells, an amplified proximal-region band of 59 nt was clearly evident in these silenced clones, including SW13(vim$^-$)-52, whose proviral DNA was methylated (Fig. 4B). By a comparison of the PCR bands, more amplification was detected using a primer set of 59 nt than 86 nt in the GFP-silenced clones SW13(vim$^-$)-31 and -52 and C33A-3 and -13 (Fig. 4B). These results suggest that short transcripts had ceased elongation at between 60 and 86 nt after initiation in these GFP-silenced clones. This indicates that the major barrier to gene silencing in Brm-deficient cells does not occur at the transcriptional initiation step because a premature termination of proviral gene transcription is clearly detectable. To detect intact short transcripts of 60 to 86 nt, we employed an RNase protection assay and analyzed some sorted clones. We designed an RNA probe complementary to the region between positions −117 and +86 of the LTR (the transcription start site is at position +1) and containing a noncomplementary 32-nt sequence at its 5′ end (Fig. 1A). As a size control for these short transcripts, we constructed an expression cassette for the 62-nt TAR element stem-loop region of HIV-1 transcripts driven by a mouse polymerase III-type U6 promoter (pmU6-62nt) and transduced this cassette into 293FT cells. For the detection of short transcripts, we collected small RNA fractions (under 200 nt) and performed an RNase protection assay with these clones. As shown in Fig. 4C, we observed a distinct single protected band of about 60 nt in the GFP$^+$ clone SW13(vim$^-$)-6 and in the GFP$^-$ clone SW13(vim$^-$)-31. This result shows that this short transcript had been generated shortly after the TAR stem-loop structure in GFP$^-$ clones.

To further examine the role of Brm in Tat-independent HIV-1 proviral transcription, we transfected a Brm, Brm-KR (a dominant negative Brm), or empty vector into the GFP-silenced clones (see Fig. S5A in the supplemental material). As shown in Fig. 5 and Fig. S5B in the supplemental material, we observed a low-level but clear induction of GFP expression in nearly the entire population of SW13(vim$^-$)-31 cells and some other clones only when transfected with wild-type Brm, indicating that the ATPase activity of Brm is essential for leaky transcriptional elongation to occur in the absence of Tat. In contrast, the induction of GFP expression was not observed in clones such as SW13(vim$^-$)-52 when transfected with wild-type Brm. Interestingly, clone 52 was shown to be a rare clone, where frequent CpG methylation was detected around the proviral 5′ LTR region (see Fig. S4 in the supplemental material). These results suggest that the responsiveness to Brm is dependent upon each specific proviral integration site and further that several kinds of epigenetic chromatin modifications could have accumulated in the promoter during each cellular expansion after GFP$^+$ cell sorting.

Brm-type SWI/SNF is recruited to the HIV-1 promoter region and alters the chromatin structure around the HIV-1 promoter. We next conducted a ChIP assay to examine whether the Brm-type SWI/SNF complex is recruited to the HIV-1 promoter in vivo. The 5′ LTR portion of HIV-1 proviral DNA was amplified by PCR (Fig. 6A). As the positive control for this assay system, we used the CD44 promoter region where SWI/SNF complexes are recruited, and as a negative control, we utilized the GAPDH promoter region at which AP-1 and SWI/SNF complexes are not recruited (Fig. 6B) (9). In this assay, we used the GFP-expressing clone HeLa-S3-4, which harbors a single proviral copy. We found from this analysis that Brm was recruited around the HIV-1 promoter site. Consistently, it has been shown that BAF155, which has been reported to be a core component for the SWI/SNF complex, is also recruited around the HIV-1 promoter site (21). These results suggest that Brm will be recruited to the HIV-1 promoter as an SWI/SNF complex. We found that the alternative catalytic subunit of the SWI/SNF complex, BRG1, is also recruited to the HIV-1 promoter, as was seen in CD44 promoter region. Whereas we cannot currently explain why recruited

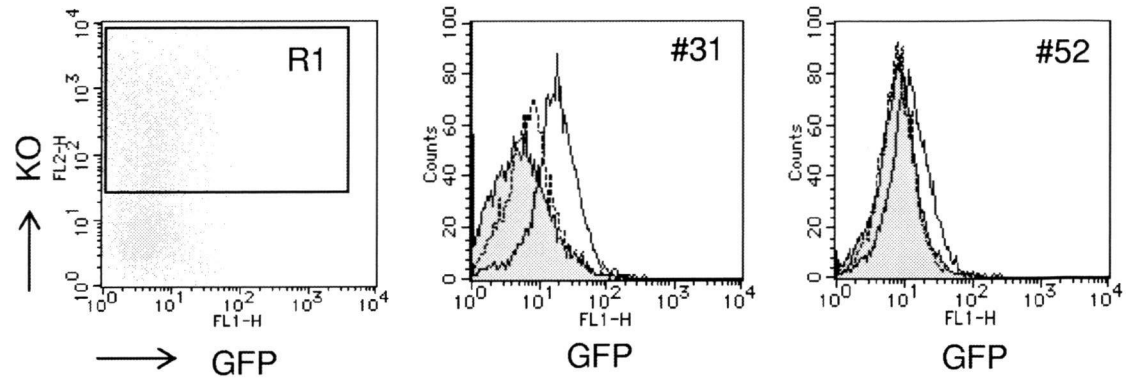

FIG. 5. Exogenous Brm transduction of GFP-silenced clones. SW13(vim$^-$) clones were transfected with vectors carrying Brm and Brm-KR as well as a control plasmid (con). At 2 days after transfection, KO-positive cells (R1 gated) were sorted, and their GFP expression profiles were analyzed by flow cytometry. Brm-transduced cells are indicated by the bold line, Brm-KR-transduced cells are indicated by the dotted line, and nontransduced parental clones are indicated by the gray line.

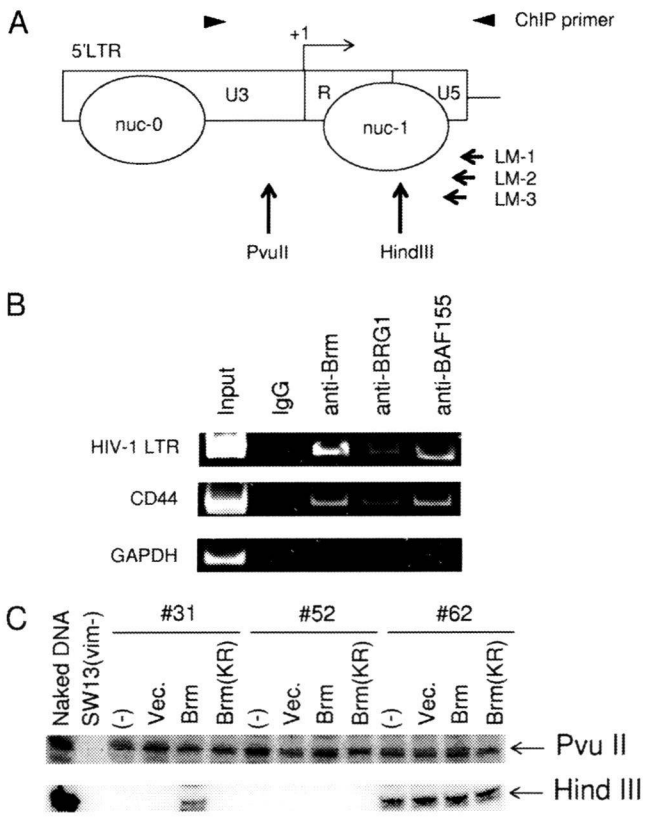

FIG. 6. Analysis of the HIV-1 LTR chromatin structure. (A) Map of the restriction sites and positions of nucleosomes (nuc-0 and nuc-1) in the HIV-1 LTR. The positions of ligation-mediated (LM) PCR primers are shown. The arrowheads indicate the PCR primer set used for the ChIP assay. (B) ChIP assay around the HIV-1 promoter site in the HeLa-S3-4 clone. Normal rabbit immunoglobulin G (IgG) was used as an antibody control. The PCR products were separated by polyacrylamide gel electrophoresis and stained with SYBR green I. Analysis of the GAPDH promoter was performed as a negative control, and analysis of the CD44 promoter was performed as a positive control. (C) Restriction enzyme accessibility assay of the HIV-1 LTR. Nuclei were isolated from untreated clones SW13(vim$^-$)-31, -52 and -62 and transfected with vectors expressing Brm, Brm-KR, or a control vector (Vec.). As a positive control, naked genomic DNA was purified from SW13(vim$^-$)-52 and then digested with PvuII or HindIII.

BRG1 does not seem to activate the transcription of this promoter, a similar selective activation potential by the Brm-type SWI/SNF complex was observed previously for the *villin* promoter (36).

The chromatin structure and the accessibility of a promoter region to host transcriptional factors are important for successful transcription. Importantly, it was previously reported that the displacement of a positioned nuc-1 downstream of a transcriptional start site is a key process for the successful transcriptional elongation of the HIV-1 provirus (28, 29). Hence, to assess the status of nuc-1 in our current analyses, we conducted a restriction enzyme accessibility assay using some of our selected GFP$^+$ and GFP$^-$ SW13(vim$^-$) clones. After the isolated nuclei were separately treated with the restriction enzymes shown in Fig. 6A, DNA was purified from them, and a primer extension reaction was performed using LM-1 as the primer (Fig. 6A). After linker ligation, PCR was performed using the sequence complementary to the linker and LM-2 as the primer pair. The degree of digestion was finally measured by a primer extension reaction using ^{32}P-labeled LM-3 as the primer (ligation-mediated PCR). In all of the GFP$^+$ and GFP$^-$ clones analyzed herein, the PvuII site present outside of the positioned nucleosomes was equally susceptible to digestion by this enzyme. However, the HindIII site that is present in nuc-1 was much more resistant to HindIII digestion in GFP$^-$ clones [SW13(vim$^-$)-31 and -52] than the GFP$^+$ clone SW13(vim$^-$)-62 (Fig. 6C). These results indicate that the nuc-1 structure of the GFP$^-$ clones in Brm-deficient cells is more rigid. Next, we tested whether these rigid nuc-1 structures are released following the induction of exogenous Brm. We transfected the Brm expression plasmid into SW13(vim$^-$) clones harboring provirus, and 48 h after transfection, we harvested the nuclei from transfected cells and assessed the nuc-1 structure using a restriction enzyme accessibility assay. The extent of digestion of the HindIII site in SW13(vim$^-$)-62 and -52 cells was unaltered by the exogenous transduction of Brm and Brm-KR. In contrast, the digestion of the HindIII site in SW13(vim$^-$)-31 was increased only when exogenous Brm was induced. These data are consistent with data from our flow cytometric analysis showing that GFP expression levels were unchanged when exogenous Brm was transduced into the

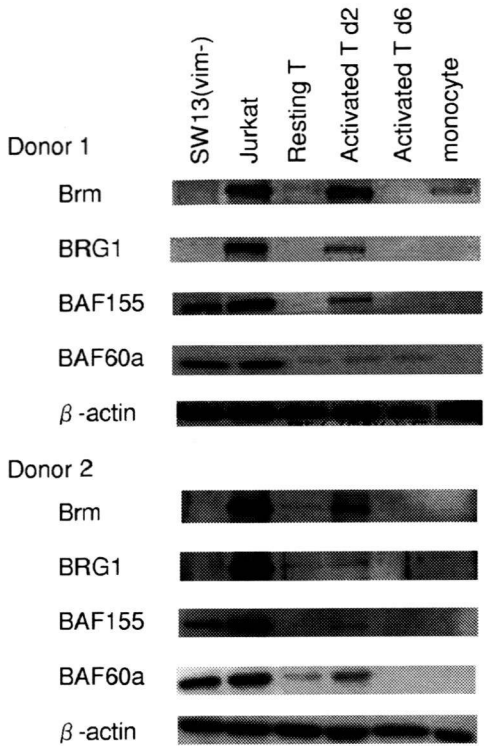

FIG. 7. Purification and characterization of resting CD4$^+$ T cells from a healthy donor. Shown is Western blotting of components of the SWI/SNF complex in resting CD4$^+$ T cells, activated CD4$^+$ T cells, and some human cancer cell lines. Brm and other components of SWI/SNF complexes were immunoblotted at 0, 2, and 6 days after cellular activation with anti-CD3 and anti-CD28 monoclonal antibodies.

clones SW13(vim$^-$)-62 and -52 (Fig. 5 and see Fig. S5B in the supplemental material). These results provide evidence that the Brm-type SWI/SNF complex is often successfully disrupting the nuc-1 structure to support transcriptional elongation and also that the extent of the reliance of HIV-1 provirus elongation upon Brm-type SWI/SNF is dependent upon the integration site of this provirus.

Brm expression levels are strongly suppressed in resting CD4$^+$ T cells. To determine the status of the SWI/SNF complex in natural host cells of HIV-1, we analyzed the expression levels of Brm and of other components of this complex in human T cells and monocytes. Resting CD4$^+$ T cells from PBMCs from healthy donors were purified by sorting the populations that expressed high levels of CD4 but no HLA-DR, a representative activation marker, whereas monocytes were purified from a CD4-dull fraction (see Fig. S6 in the supplemental material). One-half of the resting CD4$^+$ T cells obtained were further cultured in the presence of anti-CD3 and anti-CD28 to obtain activated T cells. By Western blotting (Fig. 7), it was found that the expression levels of the Brm, BRG1, BAF60a, and BAF155 subunits of the SWI/SNF complex in resting CD4$^+$ T cells were very low in two healthy donors. Importantly, activated CD4$^+$ T cells transiently induced Brm and other subunits of the SWI/SNF complex at 2 days after activation, and these subunits were then downregulated at 6 days after activation. In the case of monocytes, all of the subunits of the SWI/SNF complex examined were at marginal levels. For HIV patients undergoing highly active antiretroviral therapy (HAART) treatments, it was previously reported that cells latently infected with HIV-1 are detected principally in resting CD4$^+$ T cells that had been infected during the transition from an activated to a resting state (10). Our current result suggests the possibility that Brm plays important roles in the early Tat-independent phase of HIV-1 transcription in reactivated CD4$^+$ T cells in these patients.

Brm knockdown suppresses HIV production in ACH-2 cells. To examine whether the Brm protein is required for the reactivation of HIV-1 proviral expression from lymphocytic cells latently infected with HIV-1, we used the ACH-2 cell line as latently infected model cells. The ACH-2 cell line was derived from a T-lymphocytic parental cell line (CEM) that was latently infected with intact HIV and has been used extensively as model cell system for HIV latency and activation (22). In unstimulated ACH-2 cells, only a marginal basal level of RNA synthesis is detected, which consists predominantly of multiply spliced transcripts coding for regulatory proteins (22). Since ACH-2 cells express the Brm protein, we transduced cells with a short hairpin RNA against Brm (shBrm) expression retroviral vector into ACH-2 cells and established stable transductants by drug selection. The expression level of Brm was significantly reduced in ACH-2 cells transduced with the shBrm vector compared with those in cells transduced with a control vector (Fig. 8A). After stimulation with TNF-α, we examined HIV production in the culture medium from these transduced ACH-2 cells. To minimize reinfection after TNF-α stimulation, we added azidothymidine, an RT inhibitor, into medium prior to TNF-α stimulation. When p24 ELISA was performed, levels of HIV particles were not different between parental ACH-2 cells and cells expressing control short hairpin RNA (shRNA). On the other hand, the production of HIV-1 particles from shBrm-transduced ACH-2 cells showed significantly suppressed production compared with that of ACH-2 cells expressing control shRNA during 24 h after TNF-α stimulation (Fig. 8B).

We also determined the expression levels of endogenous *gag* proteins by Western blotting using anti-p24 antiserum. Although the accumulated amounts of the p24^{gag} protein are only slightly lower in cells expressing shBrm, the expression levels of its precursor, p55, were clearly lower in shBrm-transduced ACH-2 cells than in those expressing control shRNA (Fig. 8C). These results also support that Brm is necessary to reactivate proviral expression from latently infected ACH-2 cells.

DISCUSSION

To examine whether the Brm-type SWI/SNF complex is required for reporter gene transcription from the HIV-1 LTR in the absence of the Tat protein, we analyzed cellular clones transduced with HIV-1-based vectors carrying either LacZ or GFP (Fig. 1A). As was previously seen in MLV-based vector transduction experiments, we observed that LacZ reporter expression from an HIV-1-based vector was promptly and specifically silenced in Brm-deficient human tumor cell lines and that transduced cellular clones derived from these populations frequently formed mosaic colonies (mixture of both LacZ$^-$ and LacZ$^+$ cells) (Fig. 1B). Although the mosaic colony assay using the LacZ reporter gene is a convenient and sensitive

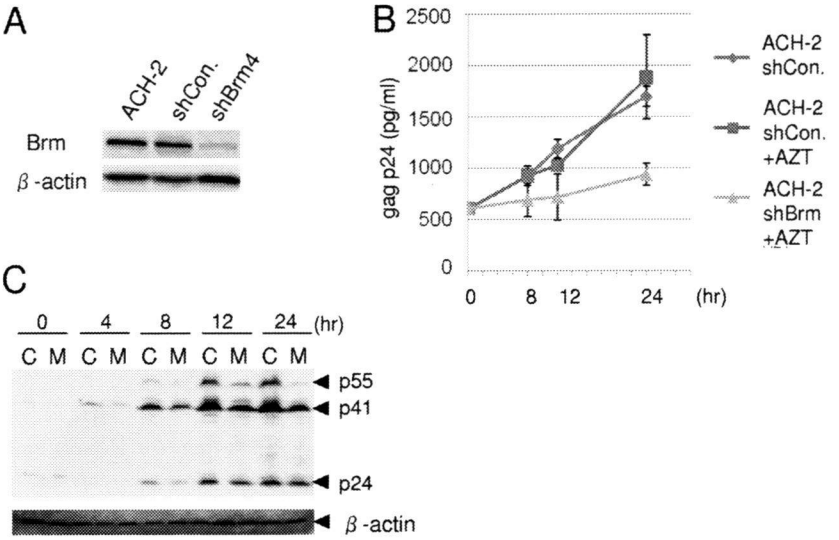

FIG. 8. Brm is required for the induction of HIV production from ACH-2 cells stimulated with TNF-α. (A) Expression levels of Brm in parental ACH-2 cells or those transduced with a retroviral vector expressing shBrm or control shRNA (shCon.). β-Actin was used for the internal control. (B) Kinetics of HIV production from these ACH-2 cells. Culture media were collected by centrifugation at 0, 8, 12, or 24 h after TNF-α (10 ng/ml) stimulation. $p24^{gag}$ antigen was detected by ELISA for the quantification of HIV particles. AZT, azidothymidine. (C) Expression of *gag* proteins in ACH-2 cells expressing shBrm (M) or control shRNA (C). Cellular pellets obtained in B were analyzed by Western blotting using anti-p24 antiserum.

method for detecting gene silencing, it is not sufficient to analyze either the clonal differences between the integrants in detail or the reversibility of these silencing events. When single cells transduced with GFP vectors were sorted for GFP^+ cells at 1 day after transduction and clonally expanded, we were able to assess the proviral gene expression profile of each integrant. Notably, in Brm-deficient cells, we frequently found GFP-silenced clones and also variegated clones that formed broad GFP expression patterns. Importantly, also, a subpopulation of GFP^- cells in this clonal culture reexpressed GFP, suggesting that silencing is reversible in cellular clones that show such broad GFP expression profiles.

It is very significant that silencing mechanisms in Brm-deficient cell lines appear to differ between MLV-based and HIV-1-based vectors. We previously reported that the silencing of an MLV-based vector in Brm-deficient cells was at the transcriptional initiation level and is caused by the recruitment of YY-1 and HDAC1/2 to the LTR region. In our current study, we have found that silencing is due mainly to the strong blockage of elongation as a result of a Brm deficiency (Fig. 4). Our analysis by RT-PCR (Fig. 4B) and RNase protection assays (Fig. 4C) reveals that proviral transcription is abortively terminated at around 60 nt in GFP-silenced clones. Here, however, we cannot exclude the possibility that the short transcript was a product of being processed from longer transcripts by digestion with exonucleases from their 3′ ends. We also show that inefficient elongation is at least partly caused by a failure in the displacement of nuc-1 downstream of the transcriptional start site of the 5′ LTR. Unlike the situation for GFP^+ clones, nuc-1 was not remodeled in GFP^- clones such as SW13(vim^-)-31 (Fig. 6C). We found that the introduction of exogenous Brm into these cells leads to a recovery of GFP expression and that this is associated with the efficient remodeling of nuc-1 in transduced clones. In several other GFP-silenced clones analyzed by flow cytometry, the GFP expression levels were also found to be recovered to various degrees by the transduction of exogenous Brm (see Fig. S5B in the supplemental material). These results suggest that Brm is required for the displacement of nuc-1 during proviral elongation in the absence of Tat. The different recovery levels of GFP expression in each integrant may be due to epigenetic changes around the promoter region that had accumulated during the course of cellular cloning over 3 weeks. By use of ChIP analysis, we demonstrated that Brm is clearly recruited to the HIV-1 LTR in a GFP-expressing HeLa-S3 transductant clone (Fig. 6B). Since BAF155 is also recruited to the HIV-1 LTR, Brm is probably recruited to the promoter as a part of an SWI/SNF complex. We also found that BRG1 is recruited to the HIV-1 LTR. Given that LacZ and GFP expression levels were stable in a BRG1-deficient cell line, H1299 (Fig. 1C and see Fig. S2 in the supplemental material), we think that the recruited BRG1 would not have a significant transactivating function at the HIV-1 LTR in the absence of Tat.

It was reported previously that latent HIV-1 proviruses are present in resting $CD4^+$ T cells of patients undergoing HAART (14). It is further believed that HIV-1 is unable to replicate efficiently in resting memory T cells because there are several viral infection and replication blocks in these cells (10). Hence, latent infection would need to have been established in resting memory T cells originating from activated T cells that were infected with HIV-1 during the process of their inactivation. Whereas latently infected cells produce little HIV-1 proviral mRNA in patients with HAART (2, 3, 7, 12), it was previously reported that abortive transcripts of about 60 nt are detectable in resting T cells from AIDS patients undergoing HAART (14). Interestingly, we show from our present data that Brm and some other components of the SWI/SNF complex, which are marginal in resting $CD4^+$ T cells, are transiently induced when they are activated by CD3 and CD28 costimulation (Fig. 7). These observations suggest that the lack

of expression of the Brm-type SWI/SNF complex would be one of the major causes of the attenuated HIV-1 proviral expression observed in resting CD4$^+$ T cells.

In the presence of Tat, stochastic expression patterns of HIV were observed previously by several groups (8, 19, 32–34). For example, it was previously reported by Weinberger et al. that Tat stochastics appear to be sufficient to generate phenotypic bifurcation (32). Here, it is assumed that there is an initial or preexisting Tat concentration of 5 to 50 molecules in the cell, which is necessary to generate phenotypic bifurcation according to predictions in silico. In our study, on the other hand, stochastic gene expression from the HIV LTR was observed in the complete absence of Tat. Weinberger et al. analyzed the expression of an LTR-GFP control HIV vector (LG) that does not produce Tat at all and concluded that their GFP levels in Jurkat cells (competent for Brm) are low and stable, which is basically consistent with data from our studies using HeLa-S3 and H1299 cell lines, which are also competent for Brm. Importantly, when host cells lacked Brm, we always observed frequent variegation in HIV LTR expression in the absence of Tat. Because the natural HIV host cells in latent infection, resting CD4$^+$ T cells, contain marginal levels of Brm (Fig. 7) and also because HIV production from a T-lymphocyte cell line latently infected with HIV, ACH-2, was strongly suppressed by knocking down Brm (Fig. 8), our observations reveal that a lack of Brm would limit and fluctuate proviral RNA elongation and further that HIV expression would be variegated in this earliest stage in these host cells. Such stochastic fluctuations in HIV expression in the absence of Tat would be further amplified by a Tat-mediated positive transcriptional feedback loop (32–34) after the Tat protein has been sufficiently accumulated. Concerning this transcriptional regulation in the earliest stage, there are important analyses of *cis* elements (8) and the status of histone modification (19) in the HIV LTR that were reported previously. In our current analysis, the Brm-type SWI/SNF complex was shown to be involved mainly in transcriptional elongation. However, it is possible that this complex would have some contribution to the regulation of transcriptional initiation together with host factors such as SP-1 (8) and HP-1-alpha as well as histone-modifying enzymes (19).

Interestingly, it was previously reported that the Tat-mediated activation of the HIV-1 promoter requires the SWI/SNF complex as a coactivator (6, 15, 27). Our current data indicated that the Brm-type SWI/SNF complex is necessary for long-transcript synthesis in the absence of Tat. These observations indicate that SWI/SNF plays essential roles in HIV-1 infection in both an early Tat-independent phase and a late Tat-dependent phase and further reveal that an understanding of the dynamism of the components and pathways involving the SWI/SNF complex during the HIV-1 infection cycle will be important to achieve in future projects.

ACKNOWLEDGMENTS

We thank Akio Adachi for providing the NL432 HIV-1 plasmid and also Sayoko Kawaura and Aki Kato for assistance in preparing the manuscript. We thank the IMSUT FACS Core Laboratory for cell sorting.

This work was supported by a grant-in-aid for scientific research on priority areas and grants by the Program of Founding Research Center for Emerging and Reemerging Infectious Disease, funded by the contract research fund from the Ministry of Health, Labor, and Welfare and the Ministry of Education, Culture, Sports, Science, and Technology (MEXT) of Japan. T.M. is a recipient of funding from PRESTO.

REFERENCES

1. **Adachi, A., H. E. Gendelman, S. Koenig, T. Folks, R. Willey, A. Rabson, and M. A. Martin.** 1986. Production of acquired immunodeficiency syndrome-associated retrovirus in human and nonhuman cells transfected with an infectious molecular clone. J. Virol. **59**:284–291.
2. **Adams, M., L. Sharmeen, J. Kimpton, J. M. Romeo, J. V. Garcia, B. M. Peterlin, M. Groudine, and M. Emerman.** 1994. Cellular latency in human immunodeficiency virus-infected individuals with high CD4 levels can be detected by the presence of promoter-proximal transcripts. Proc. Natl. Acad. Sci. USA **91**:3862–3866.
3. **Adams, M., C. Wong, D. Wang, and J. Romeo.** 1999. Limitation of Tat-associated transcriptional processivity in HIV-infected PBMC. Virology **257**: 397–405.
4. **Arai, T., K. Matsumoto, K. Saitoh, M. Ui, T. Ito, M. Murakami, Y. Kanegae, I. Saito, F. L. Cosset, Y. Takeuchi, and H. Iba.** 1998. A new system for stringent, high-titer vesicular stomatitis virus G protein-pseudotyped retrovirus vector induction by introduction of Cre recombinase into stable prepackaging cell lines. J. Virol. **72**:1115–1121.
5. **Arai, T., M. Takada, M. Ui, and H. Iba.** 1999. Dose-dependent transduction of vesicular stomatitis virus G protein-pseudotyped retrovirus vector into human solid tumor cell lines and murine fibroblasts. Virology **260**:109–115.
6. **Ariumi, Y., F. Serhan, P. Turelli, A. Telenti, and D. Trono.** 2006. The integrase interactor 1 (INI1) proteins facilitate Tat-mediated human immunodeficiency virus type 1 transcription. Retrovirology **3**:47.
7. **Brooks, R., M. J. Rotheram-Borus, E. G. Bing, G. Ayala, and C. L. Henry.** 2003. HIV and AIDS among men of color who have sex with men and men of color who have sex with men and women: an epidemiological profile. AIDS Educ. Prev. **15**:1–6.
8. **Burnett, J. C., K. Miller-Jensen, P. S. Shah, A. P. Arkin, and D. V. Schaffer.** 2009. Control of stochastic gene expression by host factors at the HIV promoter. PLoS Pathog. **5**:e1000260.
9. **Fujita, S., T. Ito, T. Mizutani, S. Minoguchi, N. Yamamichi, K. Sakurai, and H. Iba.** 2008. miR-21 gene expression triggered by AP-1 is sustained through a double-negative feedback mechanism. J. Mol. Biol. **378**:492–504.
10. **Han, Y., K. Lassen, D. Monie, A. R. Sedaghat, S. Shimoji, X. Liu, T. C. Pierson, J. B. Margolick, R. F. Siliciano, and J. D. Siliciano.** 2004. Resting CD4$^+$ T cells from human immunodeficiency virus type 1 (HIV-1)-infected individuals carry integrated HIV-1 genomes within actively transcribed host genes. J. Virol. **78**:6122–6133.
11. **Haraguchi, T., T. Mizutani, N. Yamamichi, T. Ito, S. Minoguchi, and H. Iba.** 2007. siRNAs do not induce RNA-dependent transcriptional silencing of retrovirus in human cells. FEBS Lett. **581**:4949–4954.
12. **Hermankova, M., J. D. Siliciano, Y. Zhou, D. Monie, K. Chadwick, J. B. Margolick, T. C. Quinn, and R. F. Siliciano.** 2003. Analysis of human immunodeficiency virus type 1 gene expression in latently infected resting CD4$^+$ T lymphocytes in vivo. J. Virol. **77**:7383–7392.
13. **Kao, S. Y., A. F. Calman, P. A. Luciw, and B. M. Peterlin.** 1987. Anti-termination of transcription within the long terminal repeat of HIV-1 by tat gene product. Nature **330**:489–493.
14. **Lassen, K. G., J. R. Bailey, and R. F. Siliciano.** 2004. Analysis of human immunodeficiency virus type 1 transcriptional elongation in resting CD4$^+$ T cells in vivo. J. Virol. **78**:9105–9114.
15. **Mahmoudi, T., M. Parra, R. G. Vries, S. E. Kauder, C. P. Verrijzer, M. Ott, and E. Verdin.** 2006. The SWI/SNF chromatin-remodeling complex is a cofactor for Tat transactivation of the HIV promoter. J. Biol. Chem. **281**: 19960–19968.
16. **Marciniak, R. A., B. J. Calnan, A. D. Frankel, and P. A. Sharp.** 1990. HIV-1 Tat protein trans-activates transcription in vitro. Cell **63**:791–802.
17. **Marciniak, R. A., and P. A. Sharp.** 1991. HIV-1 Tat protein promotes formation of more-processive elongation complexes. EMBO J. **10**:4189–4196.
18. **Mizutani, T., T. Ito, M. Nishina, N. Yamamichi, A. Watanabe, and H. Iba.** 2002. Maintenance of integrated proviral gene expression requires Brm, a catalytic subunit of SWI/SNF complex. J. Biol. Chem. **277**:15859–15864.
19. **Pearson, R., Y. K. Kim, J. Hokello, K. Lassen, J. Friedman, M. Tyagi, and J. Karn.** 2008. Epigenetic silencing of human immunodeficiency virus (HIV) transcription by formation of restrictive chromatin structures at the viral long terminal repeat drives the progressive entry of HIV into latency. J. Virol. **82**:12291–12303.
20. **Peterlin, B. M., and D. H. Price.** 2006. Controlling the elongation phase of transcription with P-TEFb. Mol. Cell **23**:297–305.
21. **Phelan, M. L., S. Sif, G. J. Narlikar, and R. E. Kingston.** 1999. Reconstitution of a core chromatin remodeling complex from SWI/SNF subunits. Mol. Cell **3**:247–253.
22. **Pomerantz, R. J., D. Trono, M. B. Feinberg, and D. Baltimore.** 1990. Cells nonproductively infected with HIV-1 exhibit an aberrant pattern of viral RNA expression: a molecular model for latency. Cell **61**:1271–1276.

23. **Roebuck, K. A., and M. Saifuddin.** 1999. Regulation of HIV-1 transcription. Gene Expr. **8**:67–84.
24. **Schroder, A. R., P. Shinn, H. Chen, C. Berry, J. R. Ecker, and F. Bushman.** 2002. HIV-1 integration in the human genome favors active genes and local hotspots. Cell **110**:521–529.
25. **Singh, M. K., and C. D. Pauza.** 1992. Extrachromosomal human immunodeficiency virus type 1 sequences are methylated in latently infected U937 cells. Virology **188**:451–458.
26. **Stevens, M., E. De Clercq, and J. Balzarini.** 2006. The regulation of HIV-1 transcription: molecular targets for chemotherapeutic intervention. Med. Res. Rev. **26**:595–625.
27. **Treand, C., I. du Chene, V. Bres, R. Kiernan, R. Benarous, M. Benkirane, and S. Emiliani.** 2006. Requirement for SWI/SNF chromatin-remodeling complex in Tat-mediated activation of the HIV-1 promoter. EMBO J. **25**: 1690–1699.
28. **Van Lint, C., S. Emiliani, M. Ott, and E. Verdin.** 1996. Transcriptional activation and chromatin remodeling of the HIV-1 promoter in response to histone acetylation. EMBO J. **15**:1112–1120.
29. **Verdin, E., P. Paras, Jr., and C. Van Lint.** 1993. Chromatin disruption in the promoter of human immunodeficiency virus type 1 during transcriptional activation. EMBO J. **12**:3249–3259.
30. **Wang, W., Y. Xue, S. Zhou, A. Kuo, B. R. Cairns, and G. R. Crabtree.** 1996. Diversity and specialization of mammalian SWI/SNF complexes. Genes Dev. **10**:2117–2130.
31. **Wei, P., M. E. Garber, S. M. Fang, W. H. Fischer, and K. A. Jones.** 1998. A novel CDK9-associated C-type cyclin interacts directly with HIV-1 Tat and mediates its high-affinity, loop-specific binding to TAR RNA. Cell **92**:451–462.
32. **Weinberger, L. S., J. C. Burnett, J. E. Toettcher, A. P. Arkin, and D. V. Schaffer.** 2005. Stochastic gene expression in a lentiviral positive-feedback loop: HIV-1 Tat fluctuations drive phenotypic diversity. Cell **122**:169–182.
33. **Weinberger, L. S., R. D. Dar, and M. L. Simpson.** 2008. Transient-mediated fate determination in a transcriptional circuit of HIV. Nat. Genet. **40**:466–470.
34. **Weinberger, L. S., and T. Shenk.** 2007. An HIV feedback resistor: auto-regulatory circuit deactivator and noise buffer. PLoS Biol. **5**:e9.
35. **Wu, X., Y. Li, B. Crise, and S. M. Burgess.** 2003. Transcription start regions in the human genome are favored targets for MLV integration. Science **300**:1749–1751.
36. **Yamamichi, N., K. Inada, C. Furukawa, K. Sakurai, T. Tando, A. Ishizaka, T. Haraguchi, T. Mizutani, M. Fujishiro, R. Shimomura, M. Oka, M. Ichinose, Y. Tsutsumi, M. Omata, and H. Iba.** 2009. Cdx2 and the Brm-type SWI/SNF complex cooperatively regulate villin expression in gastrointestinal cells. Exp. Cell Res. **315**:1779–1789.
37. **Yamamichi, N., K. Inada, M. Ichinose, M. Yamamichi-Nishina, T. Mizutani, H. Watanabe, K. Shiogama, M. Fujishiro, T. Okazaki, N. Yahagi, T. Haraguchi, S. Fujita, Y. Tsutsumi, M. Omata, and H. Iba.** 2007. Frequent loss of Brm expression in gastric cancer correlates with histologic features and differentiation state. Cancer Res. **67**:10727–10735.
38. **Yamamichi-Nishina, M., T. Ito, T. Mizutani, N. Yamamichi, H. Watanabe, and H. Iba.** 2003. SW13 cells can transition between two distinct subtypes by switching expression of BRG1 and Brm genes at the post-transcriptional level. J. Biol. Chem. **278**:7422–7430.
39. **Zhang, Z., A. Klatt, D. S. Gilmour, and A. J. Henderson.** 2007. Negative elongation factor NELF represses human immunodeficiency virus transcription by pausing the RNA polymerase II complex. J. Biol. Chem. **282**:16981–16988.

AIDS RESEARCH AND HUMAN RETROVIRUSES
Volume 25, Number 9, 2009

DOI: 10.1089/aid.2009.0036

Short Communication: Generation of Recombinant Monoclonal Antibodies against an Immunodominant HLA-A*2402-Restricted HIV Type 1 CTL Epitope

Jun-ichi Nunoya,[1] Toshihiro Nakashima,[2] Ai Kawana-Tachikawa,[1] Katsuhiro Kiyotani,[3] Yuji Ito,[4] Kazuhisa Sugimura,[4] and Aikichi Iwamoto[1,5,6]

Abstract

Molecular interaction between the peptide/MHC class I complexes (pMHCs) and T cell receptor (TCR) is fundamental to the effector function of cytotoxic T lymphocytes (CTLs). Monoclonal antibody against pMHC with TCR-like specificity is a possible research tool for the antigen presentation. However, it is notoriously difficult to isolate monoclonal antibodies against pMHCs by the conventional hybridoma technique. To isolate monoclonal antibodies against an immunodominant HIV-1-derived CTL epitope in the *nef* gene, we panned phage clones from a human scFv phage display library. Eight Nef138-10/HLA-A*24(A24)-specific scFv clones were isolated and two of them (scFv#3 and scFv#27) were selected for further analysis. The clones stained A24-positive cells pulsed with Nef138-10 peptides specifically. We reconstituted humanized immunoglobulin Gs (IgGs) using a baculovirus expression system. Reconstituted IgGs kept the original specificities of the parental scFvs. The dissociation constants were 23 μM and 20 μM by Biacore, respectively. This is the first report of a successful generation of monoclonal antibodies against an HIV-1 CTL epitope loaded on an MHC class I molecule.

Cellular immune response by cytotoxic T lymphocytes (CTLs) is a critical line of host defense against human immunodeficiency virus type 1 (HIV-1).[1] The first step in the CTL-based immune response is CTL activation, which is triggered through antigen recognition by a clonotypic T cell receptor (TCR).[2,3] Rather than binding to the viral antigen itself,[4] TCR binds to a complex formed with HIV-1-derived peptides and major histocompatibility complex (MHC) class I molecules (pMHCs).[5,6] Due to viral strategies to evade immune recognition, the CTL-based immune response is only partially effective in suppressing HIV-1.[1,7] One of the mechanisms by which HIV-1 circumvents CTL activities is through downregulation of MHC class I molecules by the viral Nef protein.[8] Emergence of escape mutations that alter pMHC binding or recognition is another viral strategy to disrupt the CTL-based immune response.[9,10] We previously reported that stereotypic Y to F (Y139F) substitution at the second position in an immunodominant HLA-A*2402(A24) restricted CTL epitope in the Nef protein (Nef138-10; RYPLTFGWCF) has an escape phenotype and is becoming widespread in the Japanese population.[11]

To understand cellular immune responses against HIV-1 infection, both antigen presentation and cellular responses should be analyzed. A decade ago, Altman *et al.* developed a system to analyze and evaluate the phenotype of antigen-specific T lymphocytes using pMHC tetramers.[12] However, relatively few studies have been performed to examine antigen presentation at cellular and molecular levels. For example, pMHCs derived from infecting HIV-1 have been analyzed indirectly by mass spectrometry and Cr release assays.[13,14] Lack of a suitable reagent has precluded the direct visualization and quantification of pMHCs derived from infecting HIV-1. Antibodies against HIV-1-specific pMHCs could be a useful tool to analyze antigen presentation both qualitatively

[1]Division of Infectious Diseases, Advanced Clinical Research Center, The Institute of Medical Science, The University of Tokyo, Tokyo, Japan.
[2]Division 2, First Research Department, Kikuchi Research Center, The Chemo-Sero-Therapeutic Research Institute, Kumamoto, Japan.
[3]Department of Virology, Graduate School of Biomedical Sciences, Hiroshima University, Hiroshima, Japan.
[4]Department of Bioengineering, Faculty of Engineering, Kagoshima University, Kagoshima, Japan.
[5]Research Center for Asian Infectious Diseases, The Institute of Medical Science, The University of Tokyo, Tokyo, Japan.
[6]Department of Infectious Diseases and Applied Immunology, Research Hospital, The Institute of Medical Science, The University of Tokyo, Tokyo, Japan.

and quantitatively, and the molecular interaction between pMHC and their ligands. In other studies, monoclonal antibodies against pMHCs have been isolated for specific combinations of peptides and MHC class I molecules.[15,16] In earlier studies using hybridoma technology, we attempted to isolate pMHC antibodies but failed. Technical difficulties of raising antibodies against pMHCs using a conventional hybridoma technique has led to the development of phage display techniques to isolate pMHC-specific antibodies.[17,18] We and others have constructed large phage display libraries that can be used to isolate rare antibodies.[19–21] In recent years, several recombinant antibodies against pMHC with TCR-like specificity have been isolated from similar human antibody libraries.[18,22–24] To investigate the mechanism for the escape phenotype associated with the Nef138-10 epitope at a molecular level, we tried to raise monoclonal antibodies against the epitope using the phage display technique.

We produced soluble Nef138-10/A24 and Env584-11/A24 using a Sendai virus expression system. These molecules were purified from the supernatant, and biotinylated with BirA enzyme as described previously.[25] To select Nef138-10/A24 antibodies, we used pooled human single-chain fragment variable (scFv) phage display libraries.[19] This pooled scFv library consists of four scFv library Vγ–Vλ, Vγ–Vκ, Vμ–Vκ, and Vμ–Vλ, containing 1.1×10^8, 2.1×10^8, 8.4×10^7, and 5.3×10^7 independent clones, respectively. To remove phages that might bind nonspecifically to the beads, the library (1.0×10^{12} transforming units) was incubated with streptavidin-coated magnetic beads (Dynal, Oslo, Norway) for 1 h with continuous rotation. The beads were removed and the supernatant was incubated for 1 h with 500 nM Nef138-10/A24s. Streptavidin-coated magnetic beads were incubated for 1 h with 2% skim milk/phosphate-buffered saline (PBS) and then added to the antigen/supernatant mixture. After a 15-min incubation with continuous rotation, the supernatant was removed and the beads were washed 10 times with PBS containing 0.1% Tween 20 and two times with PBS. Phages were eluted from the beads with 100 mM triethylamine (Sigma, St. Louis, MO), and the solution was immediately neutralized by the addition of 1 M Tris–HCl (pH 7.4). *Escherichia coli* strain TG1 (GE Healthcare UK Ltd.) was transduced with eluted phages and plated on a 2xYT agar plate containing 2% glucose and 100 μg/ml carbenicillin (Sigma). After overnight incubation at 30°C, all colonies were picked and cultured in a single flask with liquid medium, with the addition of helper phage M13KO7 (GE Healthcare UK Ltd.). The scFv-displayed phages were purified from the supernatant by polyethylene glycol precipitation, titrated with *E. coli* strain TG1, and used for the next round of panning.

The protocol for the second and third rounds was the same as for the first round, except that phage supernatant was incubated with a lower concentration (100 nM) of Nef138-10/A24 peptide complexes. After two and three rounds of panning the scFv phage display library with biotinylated Nef138-10/A24 and streptavidin-coated magnetic beads in solution, we achieved a 38.2- and 4200-fold enrichment, respectively, for scFvs that bind to Nef138-10/A24 (Fig. 1A).

After the third round of panning, helper phages were added to each culture of the individual colonies in order to recover phages for ELISA as described previously.[23] Briefly, 96-well maxisorp plates (Nunc, Rochester, NY) were coated with biotinylated bovine serum albumin (BSA) (1 μg/well; Vector Laboratories Inc., Burlingame, CA) overnight at 4°C, washed three times with 0.1% Tween 20/PBS (the buffer used for all subsequent washes), and incubated with streptavidin (1 μg/well; Sigma) for 1 h. Plates were washed three times, incubated with biotinylated peptide/A24 (0.5 μg/well) for 1 h, and blocked with 2% skim milk/PBS for 30 min. Plates were washed three times, incubated for 1 h with $\sim10^{10}$ phages or isolated antibodies, and washed three times. Detector antibodies were added (see figure legends) and plates were incubated for 1 h at 4°C. Plates were washed four times, and antibody binding was detected by a colorimetric detection method with a TMB reagent (Pierce Biotechnology Inc., Rockford, IL). The reaction was stopped by the addition of 0.5 M H_2SO_4. In addition, DNA fragments encoding scFv were amplified by colony PCR with primers C5E-S1 (5′-CAACG TGAAAAAATTATTATTCGC-3′) and C5E-S6 (5′-GTAAAT GAATTTTCTGTATGAGG-3′). DNA sequencing was performed using the same primers and the ABI Prism dye terminator cycle sequencing Ready Reaction kit (Applied Biosystems, Foster City, CA) on a Perkin-Elmer ABI-377 sequencer. We isolated 80 clones of scFv-displaying phages after the third round of panning and assayed them by ELISA to assess binding to Nef138-10/A24 and Env584-11/A24 (Fig. 1B). As a control, we used the monoclonal antibody W6/32, which binds to HLA-ABC molecules properly associated with a heavy chain and a β_2-microglobulin. W6/32 recognized both Nef138-10/A24 and Env584-11/A24, indicating that both peptide/A24 complexes maintained a correct conformation during the ELISA procedure (Fig. 1B, PC).

Of the 80 clones, 16 bound preferentially to Nef138-10/A24; the remainder bound to both Nef138-10/A24 and Env584-11/A24. Following *Bst*OI digestion and sequencing of the 16 scFv DNA fragments that were specific for Nef138-10/A24, we isolated eight independent clones of scFv-displaying phages. We confirmed the expression and binding specificity of each scFv clone by Western blotting and ELISA with anti E-tag antibody.

For purification and detection of soluble scFvs, we genetically converted the E-tag located at the scFv C-terminus to the tandem sequences of c-Myc and 6xHis tags. To express scFvs, *E. coli* strain TG1 transformants were cultured at 30°C. When the OD_{600} reached 0.5, expression was induced by the addition of 1 mM IPTG. Cultures were incubated for an additional 4 h at 30°C. To prepare periplasmic fractions, bacteria were collected by centrifugation and osmotically shocked with ice-cold 0.2 M Tris–HCl containing 0.5 mM EDTA and 0.5 M sucrose at pH 8.0. scFvs were purified from periplasmic extracts by affinity chromatography with HiTrap Chelating HP Column (GE Healthcare UK Ltd.). After replacing the C-terminal E-tags with c-Myc and 6xHis tags, we confirmed the expression of each scFv clone in the periplasm and supernatant using Western blotting with anti c-Myc tag antibody (data not shown). We selected scFv#3 and scFv#27 for further analysis. In ELISA with anti-c-Myc tag antibody, soluble forms of scFv#3 and scFv#27 bound specifically to Nef138-10/A24 (Fig. 1C).

To analyze the binding specificity of the two selected scFv clones toward pMHCs expressed on the cell surface, we performed flow cytometry analysis of a peptide pulsed A24-positive Epstein–Barr virus-transformed B lymphoblastoid cell line (B-LCL) previously established in our laboratory.[25] Two$\times10^6$ cells from an A24-positive B-LCL were pulsed for 20

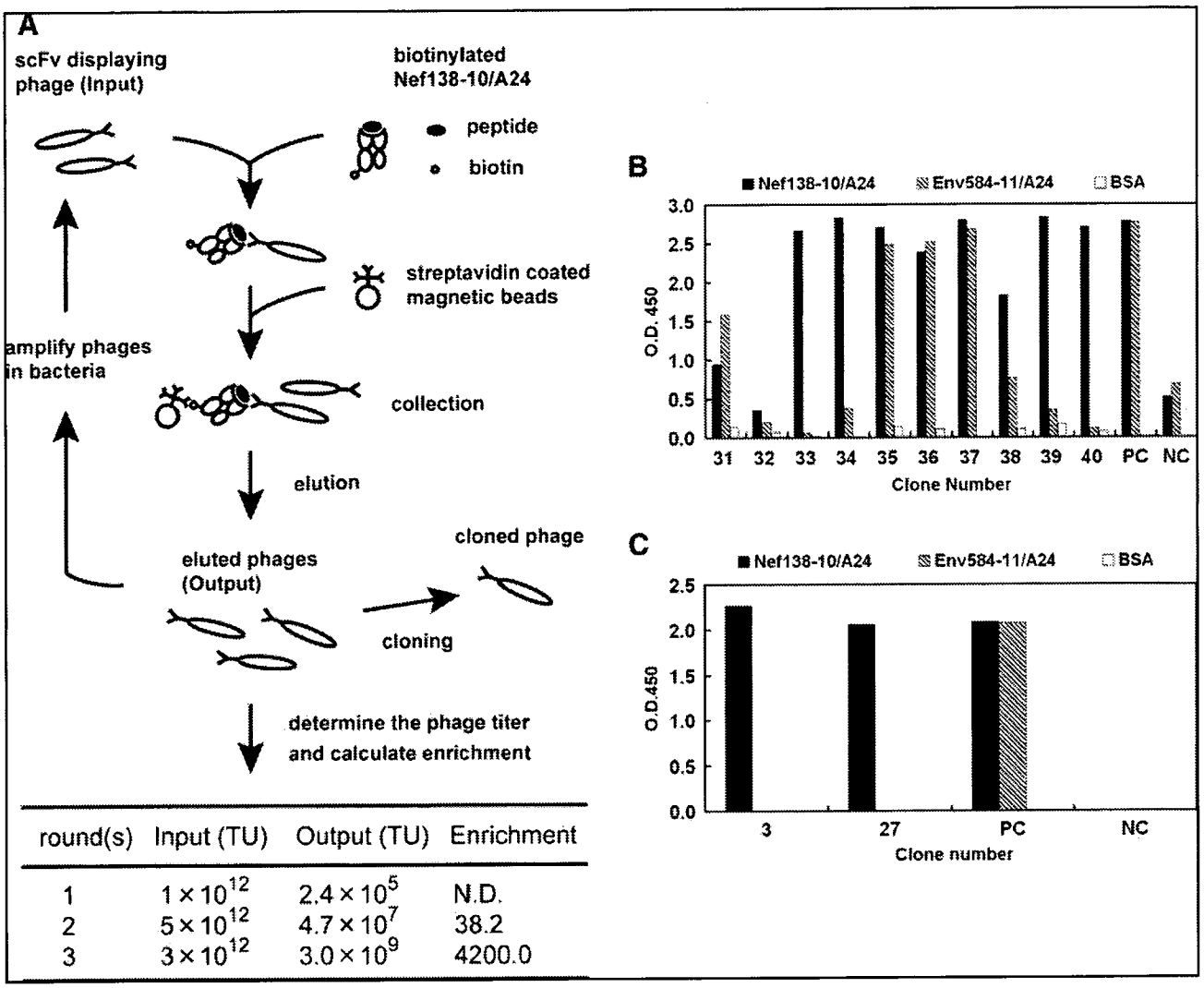

round(s)	Input (TU)	Output (TU)	Enrichment
1	1×10^{12}	2.4×10^{5}	N.D.
2	5×10^{12}	4.7×10^{7}	38.2
3	3×10^{12}	3.0×10^{9}	4200.0

FIG. 1. Isolation of scFvs directed against Nef138-10/A24. (**A**) A schematic representation of panning. The scFv-displaying phages that bind to Nef138-10/A24 were panned from a naive human scFv phage display library and collected by streptavidin-coated magnetic beads. Panning was repeated three times. The enrichment during panning was calculated from the phage titer bound to Nef138-10/A24. (**B**) Binding specificity of scFv-displaying phage clones from the phage pool after three rounds of panning. Recovered panned phages were screened in ELISA for specific binding to Nef138-10/A24 by using an HRP-conjugated anti-M13 phage antibody (GE Healthcare UK Ltd.). Each clonal phage and PBS as a negative control (NC) were assayed in duplicate for its binding to Nef138-10/A24 (filled bar), Env584-11/A24 (hatched bar), and BSA (open bar). We used an anti-HLA-ABC antibody (W6/32) as a positive control (PC), and detected the bound antibodies with HRP-conjugated antimouse immunoglobulins (Igs) antibodies (DAKO, Glostrup, Denmark). The numbers below the horizontal line indicate clones. The ordinate indicates the optical density value at 450 nm (OD_{450}). This figure shows results of typical 10 clones (scFv#31–40). We judged a clone specific binding to Nef138-10/A24, when its OD_{450} value of Nef138-10/A24 was 10 and 5 times higher than those of BSA and Env584-11/A24, respectively. (**C**) Binding specificity of scFvs expressed in the *E. coli* periplasm was analyzed by ELISA with anti-c-Myc-tag antibody (Santa Cruz Biotechnology Inc., Santa Cruz, CA).

to 24 h with 10 μM of each peptide in FCS-free RPMI. After pulsing, cells were washed three times, incubated with purified scFvs (50 μg/mL) for 1 h at 4°C, washed two times, and incubated with a biotinylated rabbit polyclonal anti-c-Myc antibody (10 μg/mL) for 1 h at 4°C. Cells were washed twice and incubated with R-phycoerythrin (PE)-conjugated streptavidin (10 μg/ml; BD Pharmingen, San Diego, CA) for 1 h at 4°C, then washed three times and fixed with PBS containing 1% paraformaldehyde. PBS containing 2% heat-inactivated normal rabbit serum (NRS) and 0.02% sodium azide was used as the diluent for all scFvs and antibodies. All washes were performed with PBS. Flow cytometry was performed using a FACSCalibur (BD Bioscience, San Jose, CA). Both scFv clones bound specifically to Nef-138-10/A24. No cross-reactivity was observed toward endogenously expressed HLA-A, HLA-B, or HLA-C molecules or toward A24-bound HIV-1 Gag28-9, HIV-1 Env584-11, or CMV pp65 complexes (Fig. 2). HLA-A, HLA-B, and HLA-C molecules were expressed equally among the cell populations used in this assay (Fig. 2, W6/32). These data suggest that the scFv#3 and scFv#27 bind specifically to

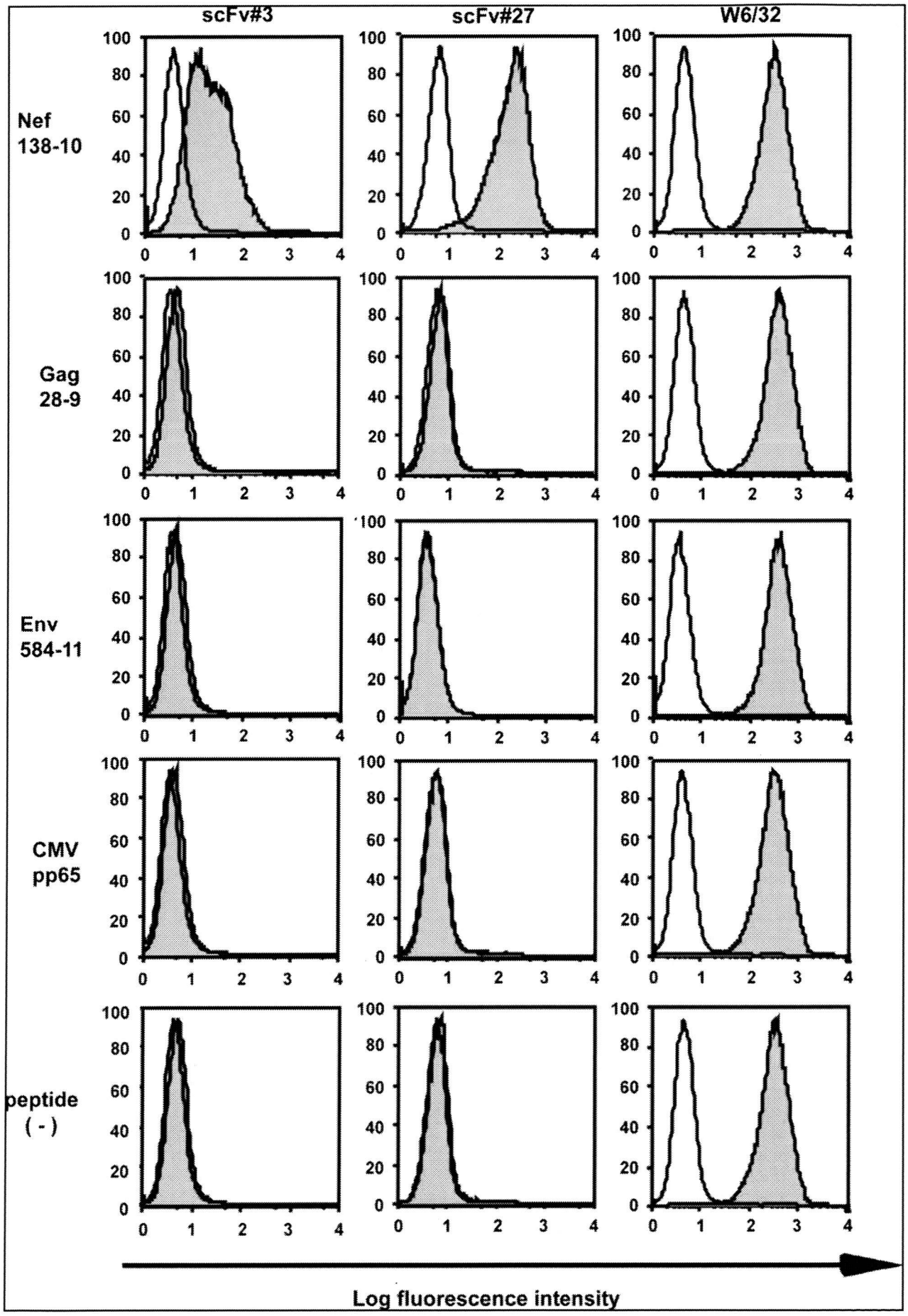
scFv#3
scFv#27
W6/32
Nef 138-10
Gag 28-9
Env 584-11
CMV pp65
peptide (-)
Log fluorescence intensity